AMERICAN UNIVERSITY OF BEIRUT

THE IMPACT OF CIGARETTE SMOKING ON TYPE I CARDIO-RENAL SYNDROME IN MALE AND FEMALE MICE

by

NADA JACQUES HABEIHCI

A thesis
submitted in partial fulfillment of the requirements
for the degree of Master of Pharmacology
to the Department of Pharmacology and Toxicology
of the Faculty of Medicine
at the American University of Beirut

Beirut, Lebanon
October, 2018

AMERICAN UNIVERSITY OF BEIRUT

THE IMPACT OF CIGARETTE SMOKING ON TYPE I CARDIO-RENAL SYNDROME IN MALE AND FEMALE MICE

by

NADA JACQUES HABEICHI

Approved by:

Dr. Zouein, Fouad, Assistant Professor — Advisor
Department of Pharmacology and Toxicology

Dr. El-Yazbi, Ahmed, Assistant Professor — Co-Advisor
Department of Pharmacology and Toxicology

Dr. Eid, Ali, Assistant Professor — Member of Committee
Department of Pharmacology and Toxicology

Dr. Eid, Assaad, Associate Professor — Member of Committee
Department of Anatomy, Cell Biology and Physiological Sciences

Date of thesis/dissertation defense: October 4, 2018

AMERICAN UNIVERSITY OF BEIRUT

THESIS, DISSERTATION, PROJECT RELEASE FORM

Student Name: _Habeichi_____Nada_____Jacques_____

● Master's Thesis ○ Master's Project ○ Doctoral Dissertation

☐ I authorize the American University of Beirut to: (a) reproduce hard or electronic copies of my thesis, dissertation, or project; (b) include such copies in the archives and digital repositories of the University; and (c) make freely available such copies to third parties for research or educational purposes.

☒ I authorize the American University of Beirut, to: (a) reproduce hard or electronic copies of it; (b) include such copies in the archives and digital repositories of the University; and (c) make freely available such copies to third parties for research or educational purposes

after: One ---- year from the date of submission of my thesis, dissertation, or project.

Two ---- years from the date of submission of my thesis, dissertation, or project.

Three ✓ years from the date of submission of my thesis, dissertation, or project.

Nada

Signature Date 14/01/2019

ACKNOWLEDGEMENT

I would like to express my deepest gratitude to my guardian angel, my advisor Dr. **Fouad A. Zouein**. I am amazingly fortunate and blessed to be your student. Thank you so much for always having my back. You stood by me in every step and gave me the guidance, strength, and support to finish my thesis. If I had a chance to repeat this experience, I would definitely choose you again and again. You were my safe haven in Lebanon and you turned my career and my life around to the better.

I would also like to give heartfelt thanks to my co-advisor Dr. **Ahmed El-Yazbi.** Your insight discussions about the thesis have been priceless. Thank you for all your support and patience with me during this year and thank you for guiding me to grow as a researcher.

A very special thank goes to the greatest research assistant, and to my best friend Dr. **Ali Mroueh**. No words can describe how much I am blessed and lucky to work with you. Thank you for the time and the effort you gave me to learn each and every research technique.

To my best friends and lab mates, Dr**. Cynthia Tanous** and **Hiam Alawassi**. My lab experience would never be the same without you by my side.

Thank you to Dr. Zouein and Dr. El- Yazbi's teams for all the fun and support. Thank you so much **Dr. Kapplan** for the explanations you gave me to understand the pathological mechanisms behind type I CRS.

I would also like to thank my family in Lebanon: Dina, Karim, Omar, Yasmeen, Ghalia, and Jaffar for their endless support.

Last but not least, my most sincere gratitude goes to **my family** especially my parents for all their sacrifices for me to grow and prosper.

AN ABSTRACT OF THE THESIS OF

Nada Jacques Habeichi for Master of Science
Major: Pharmacology and Toxicology

Title: The Impact of Cigarette Smoking On Type I Cardio-Renal Syndrome in Male and Female Mice

Overwhelming epidemiological evidence correlates cardiovascular diseases (CVDs) with acute kidney injury (AKI) and cigarette smoking (CS). CS contains thousands of carcinogenic and non-carcinogenic chemicals that play a key role in reducing cell viability in renal proximal tubular epithelial cells through acute or chronic pathological mechanisms. Myocardial infarction (MI) is a major public health concern and a leading cause of type I cardio-renal syndrome in both males and females. In this study, the impact of CS on type I cardio-renal syndrome in both genders was investigated in a mouse model of MI using 3 groups: control, MI, and MI + CS of each gender.

Histological analysis of MI+CS groups showed morphological alterations in the kidneys including glomerular retraction, proximal convoluted tubule dilatation, and interstitial fibrosis, which were significantly heightened in males when compared to the relative female subjects.

Molecularly, the pro-inflammatory cytokine IL-1β was markedly increased in males post MI+CS when compared to the control group, whereas, the anti- inflammatory cytokine IL-13 was significantly heightened in females MI following CS exposure when compared to the relative male group. The pro-fibrotic biomarkers MMP8 and α-SMA were markedly increased in MI males following CS exposure when compared to the relative female group. Of note, MMP13, CTGF tended to be non- significantly higher in MI males following CS exposure when compared to relative female mice despite a comparable increase in ROS production and DNA fragmentation.

Metabolically, NAMPT and NMRK1 were significantly increased in MI females following CS exposure when compared to relative male mice. Both SIRT1 and SIRT3 were markedly decreased in MI male following CS exposure when compared to the relative female subjects. Additionally, PARP-1 tended to be higher in MI male group following CS exposure when compared to the relative female group. Last but not least, NAD levels significantly decreased in MI male mice following CS exposure when compared to MI and control male groups. In conclusion, our findings revealed that CS exposure exacerbates MI-induced kidney damage in a gender biased manner with female mice being less susceptible to damage than relative males.

CONTENTS

ILLUSTRATIONS

Figure Page

CHAPTER I

INTRODUCTION

A. The Cardio-Renal System

Cardiovascular and renal systems are intimately related through a synergistic interrelationship in order to maintain cardio-renal homeostasis [4]. Acid-base and electrolytes equilibriums are maintained by the kidneys, whereas, the heart is responsible for providing a sufficient amount of blood to the vital organs of the body through the vasculature [5]. This bidirectional interrelationship is fine-tuned by neurohumoral activity, including sympathetic nervous system (SNS), renin-angiotensin-aldosterone system (RAAS), atrial natriuretic peptides (ANP), and baroreflex systems. Under physiological conditions following an increase in blood pressure (BP), SNS/RAAS activity is diminished while ANP production and baroreflex activation restore BP to normal range maintaining therefore the cardio-renal homeostasis [6]. The baroreflex system is divided into two integrated negative feedback systems adjusting the momentary activation of SNS and RAAS. For instance, any alteration in systolic BP is modulated by both the aortic-carotid and the cardiopulmonary baroreflex systems, allowing preservation of normal peripheral vasoconstriction, venous return, stroke volume (SV), cardiac output (CO), and renal perfusion [7]. ANP on the other hand, is increased with BP increase exerting a vasodilatory effects on the arteries and the venous system causing a decrease in systemic vascular resistance, increase in venous dilatation, and a

subsequent decrease in BP. Additionally, ANP inhibits renin secretion from the juxtaglomerular cells of the kidneys, and norepinephrine from sympathetic nerve terminals contributing to the maintenance of hemodynamic homeostasis [8]. In contrast, if BP falls, SNS and RAAS are activated, and ANP secretion is inhibited. SNS contributes to physiological long-term blood pressure regulation via the action of norepinephrine on β1 adrenoceptors. β1 is the most prominent subtype of beta-adrenoceptors in the heart enhancing upon stimulation cardiac inotropic, dromotropic, lusitropic, and chronotropic effects [9]. In the kidneys, β1 stimulation elevate renin synthesis and release; subsequently, renin convert angiotensinogen to angiotensin II, a vasoactive peptide that increase aldosterone synthesis, salt and water retention, and intravascular volume expansion mainly via its actions on the AT1R receptor [10, 11].

B. The Cardio-Renal Syndrome (CRS)

1. The Cardio-Renal Syndrome (CRS)

The Acute Decompensated Heart Failure National Registry (ADHERE) database postulated that more than 30% of patients with cardiac dysfunction are diagnosed with kidney diseases. Additionally, in a systemic review of 16 studies, 29% of patients with heart failure developed moderate and severe kidney impairment [12] [13]. Cardio-renal syndrome (CRS) is defined as a complex clinical condition in which both cardiac and kidneys dysfunction overlap [14]. Based on whether the initial injury originates in the kidneys or the heart, CRS is classified into five distinct types.

2. CRS Classifications

a. Type1 CRS

Type 1 CRS is defined as an acute cardiac dysfunction (i.e. acute myocardial infarction (AMI)) leading to an acute kidney injury (AKI).

b. Type 2 CRS

Type 2 CRS is defined as a chronic cardiac dysfunction (i.e. congestive heart failure) causing a chronic kidney disease (CKD).

c. Type 3 CRS

Type 3 CRS is defined as an AKI inducing acute cardiac disease.

d. Type 4 CSR

Type 4 CRS is defined as a CKD leading to the development of chronic cardiac dysfunction.

e. Type 5 CRS

Type 5 CRS is defined as a systemic condition such as diabetes mellitus causing a simultaneous injury in both the heart and the kidneys [15].

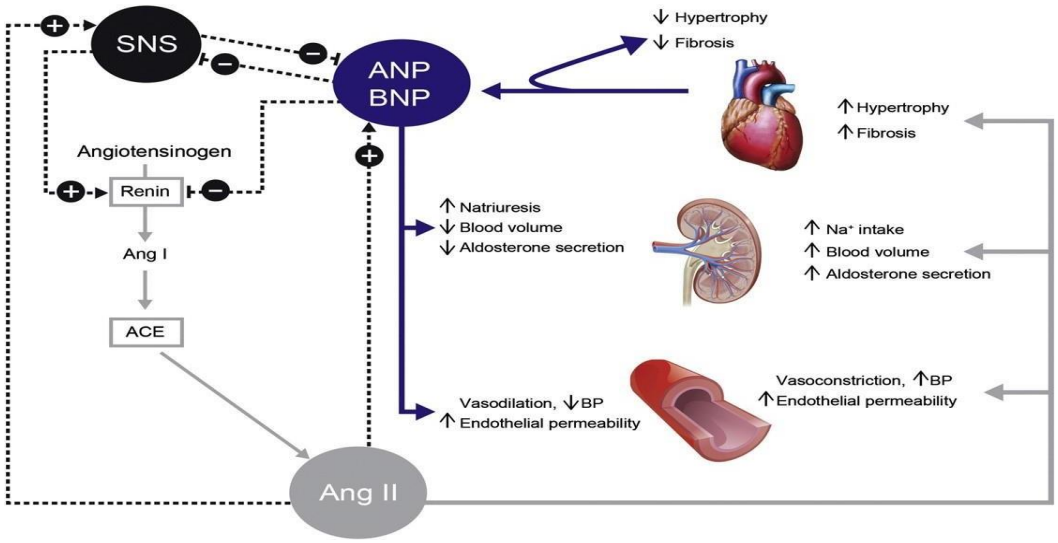

Figure 1 *Cardio-Renal System*

Schematic diagram to show how the NP system, the RAAS and the SNS interact in order to maintain cardio-renal homeostasis, and how the effects of the NP system and the RAAS on key organs are generally counter-regulatory. ACE = angiotensin converting enzyme; Ang = angiotensin; ANP = atrial natriuretic peptide; BNP = B-type natriuretic peptide; BP = blood pressure; NP = natriuretic peptide; RAAS = renin–angiotensin–aldosterone system; SNS = sympathetic nervous system [1].

C. Myocardial Infraction (MI)

1. Myocardial Infarction (MI) Prevalence:

MI is a major health concern. It generally occurs when blood flow to one or multiple areas in the heart is blocked, leading to cardiomyocytes death, followed by an alteration in the structure and function in the left ventricle (LV) of the heart defined as left ventricle (LV) remodeling [16]. According to the World Health Organization(WHO) more than 31% of cardiovascular (CVDs) related deaths are due to coronary heart diseases (CHD) [17]. The 2016 heart disease and stroke statistic estimated that one American will suffer from MI every 42

seconds [18]. The epidemiology of MI has been assessed using the influence of sex and risk factors [19]. The prevalence of MI is higher in males compared to age-matched females, and it is dramatically increasing by age in both genders [20]. Additionally, gender disparity disappears in women with reduced estrogen level post menopause [21]. For instance, in patients under 45 years of age, the male to female ratio is 10:1, dropping progressively to 2:1 in patients over 75 years of age [22].

2. Myocardial infarction (MI) risk factors:

According to TIMI risk score assessment, multiple factors including hypertension, obesity, diabetes mellitus, and cigarette smoke (CS) are identified as both dependent and independent high risk factors for MI development [19].

a. Obesity

Obesity is well-recognized as a major risk factor for cardiovascular diseases (CVDs) [23]. Epidemiological studies have demonstrated that abdominal obesity increases the incidence of MI in both genders [24, 25]. Moreover, for every 10 kg increase in body weight a 12% increase in CHD risk arise [26]. Obesity significantly correlates with hypertension, dyslipidemia, and diabetes mellitus (DM), all of which are pivotal risk factors for CHD development [27]. It is well documented that the accumulation of adipose tissues in the vessel wall plays a crucial role in obesity induced CVDs [28]. In lipid storage diseases, the transendothelial passage of low density lipoprotein (LDL), Intermediate density lipoprotein (IDL), and very-low density lipoprotein (v-LDL) from plasma into the vascular intima triggers

an inflammatory response mediated by macrophages infiltration and monocytes activation [29]. These inflammatory reactions boost the release of inflammation-related adipokines such as interleukin (IL-1), IL-6, endothelin, angiotensinogen, therefore accelerating CHD development [30, 31].

b. Diabetes Mellitus (DM)

The prevalence of CHD is very common in diabetic patients. Hyperglycemia and insulin resistance highly correlates with the overexpression of multiple pro- inflammatory cytokines including IL-1, IL-6, and tumor necrosis factor- alpha (TNF- α), all of which drastically accelerate the risk of endothelial dysfunction [32, 33]. The pro-inflammatory environment along with the high level of C reactive protein (CRP), impairs endothelial nitric oxide formation, prostacyclin synthesis, and increases the uptake of oxidized LDL in coronary arteries, therefore promoting endothelial dysfunction, atheroma plaque formation, and subsequently, increasing the risk of myocardial ischemia [34, 35]. The incidence of MI is 3.4 times higher in diabetic women and 2.5 times higher in diabetic men when compared to control subjects even after adjusting for other risk factors such as hypertension, dyslipidemia, and cigarette smoke (CS) [36]. Clinical studies revealed a 4 fold higher risk in diabetic men and 7folds higher risk in diabetic women of MI-related mortality rate when compared to non-diabetic MI populations [36, 37].

c. Hypertension

Hypertension is a common risk factor for MI [38]. Multiple epidemiological and clinical studies reported that more than 39% of MI cases are attributed to hypertension [39, 40]. The prevalence of BP is higher in men compared to age- matched women. However, this discrepancy is gradually decreasing post menopause, with a risk of hypertension increasing to 58% in women between 60-70 years old. [41-44]. Long-term increase in BP due to an over activation of SNS and RAAS can aggravate vascular endothelial dysfunction by causing changes in extracellular matrix turnover, and eventually increasing the risk of CHD development. Additionally, serious consequences of persistent elevation in BP, such as hypertrophy and interstitial fibrosis, can lead to structural and functional alteration in the left ventricle (LV) of the heart defined as left ventricular hypertrophy (LVH) [45]. If left untreated, LVH increase the risk of ischemic cardiomyopathy and subsequent heat failure development [46].

d. Cigarette smoking (CS)

A strong pre-clinical and clinical evidence highlight the involvement of CS as an independent factor in CHD development [47]. The cardiovascular risks caused by CS are tightly related to the duration of smoking and the amount of cigarettes smoked [48, 49]. Additionally, CS results in a 5 -old increase in the incidence of MI in women versus 10 folds increase in men [50]. Accumulating epidemiological studies report that CS is responsible for one in every five deaths (~ 5 million deaths/year) with a 6% to 15% association with overall healthcare costs in developed countries [51]. Moreover, smokers are estimated to exceed one

billion individual worldwide (> 10 million deaths/year) by 2025 despite the awareness of CS risks [52] [53] [54]. CS contains more than 5000 potential toxicants including amid, free radicals, oxidative gases, reactive oxygen species (ROS), and carbon monoxide among others [55]. Nicotine is a main smoking alkaloid presents in a high concentration in CS [56]. Additionally, nicotine can be acquired through active and passive smoking and it has a crucial role in CHD development [57]. Two pathological mechanisms are involved in cardiac remodeling following chronic CS; direct actions of CS on cardiac muscle including necrosis, fibrosis, myocardial ischemia, and coronary vasoconstriction, leading to metabolic and morphological changes in the heart also known as smoke cardiomyopathy. Indirect actions, by increasing the adverse effects of other comorbidities such as hypertension, dyslipidemia, and inflammatory reactions that further fuel their high risk impact on CHD development [3] [58].

3. Myocardial Infarction (MI) Pathophysiology

Despite the current pharmacological and interventional therapies and the remarkable increase in survival rates following MI (60% to ~ 90%), around 25% of MI patients still undergo adverse left ventricle remodeling [59]. Cardiac remodeling post-MI varies based on the infarct size, the healing process, and the presence or absence of comorbidities [60]. Following coronary artery occlusion, the hypoxic environment shifts ATP production to anaerobic glycolysis increasing intracellular acidosis and promoting cell death and necrosis [61]. Subsequently, dangerous associated molecule patterns (DAMPs) including DNA, RNA, heat shock proteins (HSPs), and adenosine triphosphate (ATP) are released from dying cardiomyocytes into the surrounding extracellular space. Three interchangeable phases are

involved in wound healing process following MI [16] [62]. The early inflammatory phase, mediated by the recruitment of monocytes and neutrophils to the site of injury, is initiated at the onset of MI [3]. This inflammatory response triggers monocytes differentiation into macrophages M1, resulting in fibroblast proliferation, activation of pro-inflammatory cytokines (IL-1, IL-6, TNF-a), and extracellular matrix (ECM) degradation [63]. The granulation phase is characterized by the activation of macrophages M2 including (IL- 10, TGF-B1), subsidization of inflammation, differentiation of fibroblast to myofibroblasts, and ECM deposition [64]. Fibrotic scar formation and myofibroblast survival are the hallmark of the last phase known as the maturation phase [65]. Prolonged ischemia and inflammatory response have a central impact on cardiomyocytes within both infarcted and non-infarcted areas and is proven to be detrimental in the absence of appropriate inflammatory resolution and adequate transition between remodeling phases [66]. Noteworthy, unresolved inflammation promotes progressive infarct expansion and border zone extension by inducing myocyte death and extracellular matrix (ECM) degradation [67, 68]. Additonally, upon infarction, the mechanical workload of the heart shifts to the remote uninfarcted region which responds by increasing the amount of contractile units. However, remote hypertrophied myocytes are vulnerable and dysfunctional with reduced systolic sarcoplasmic reticulum Ca release and desensitization to Ca which further exacerbate systolic dysfunction post-MI [69, 70].Wound-healing process. Three phases are identifiable in the wound-healing process that follows myocardial infarction. Inflammation phase: (1) Onset of myocardial infarction by obstruction of blood flow in coronary arteries. (2) Hypoxic environment triggers cellular necrosis and the release of DAMPs. (3) Irritated endothelium expresses adhesion molecules

and alert circulating innate immune cells. (4) Acute inflammatory response is initiated by neutrophil and monocyte recruitment, activation, and extravasation to the site of injury. (5) Pro- inflammatory environment triggers monocytes to macrophage M1 differentiation and activation. (6) Macrophages stimulate fibroblast proliferation and migration which further boost pro-inflammatory cytokines (i.e. IL-1, IL-6, and TNF-α), chemokines (i.e. MCP-1 and IL-8), release of proteinases (i.e. MMPs), and ECM degradation. Granulation phase: (7) Macrophage phagocytosis of necrotic debris and apoptotic neutrophils which triggers M2 macrophages activation. (8) M2 molecules (i.e. IL-10 and TGF-β) subside inflammation and stimulate fibroblast to myofibroblast differentiation. Myofibroblast becomes the major producer of ECM components and mediators of ECM deposition. Maturation phase: (9) Prolonged myofibroblast survival along with ECM crosslinking and fibrotic scar maturation and contraction [3].

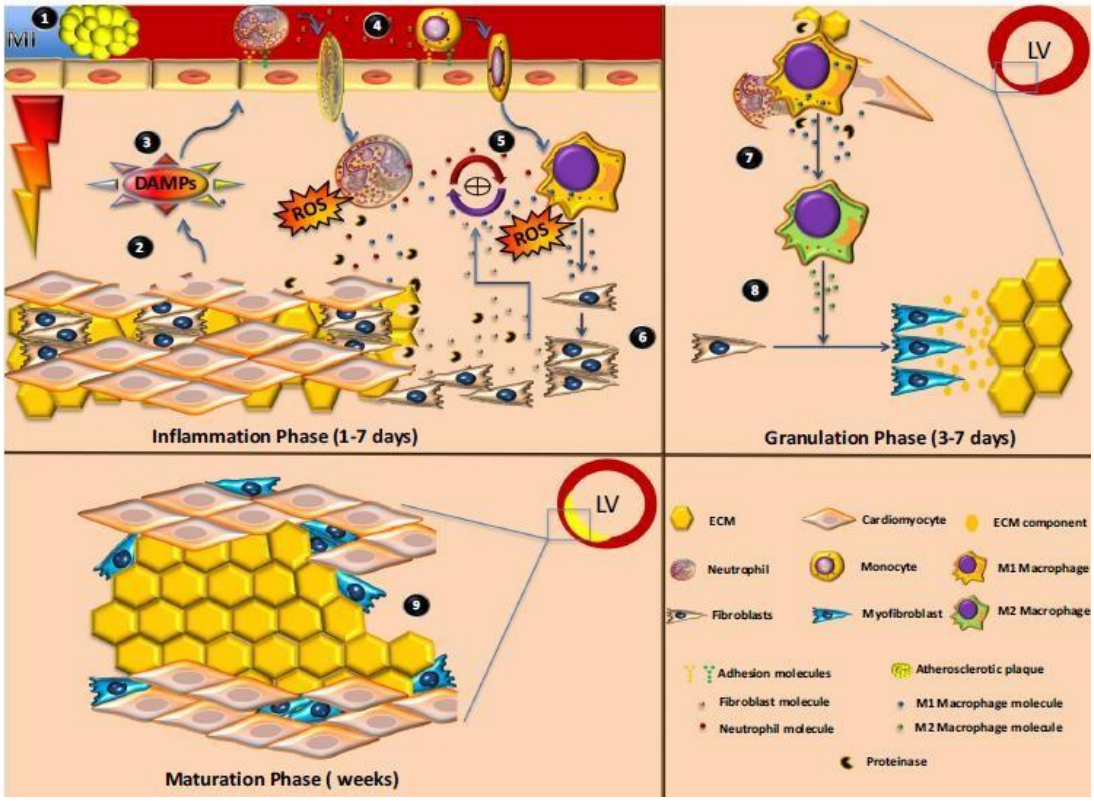

Figure 2 Wound-healing process

Three phases are identifiable in the wound-healing process that follows myocardial infarction. Inflammation phase: (1) Onset of myocardial infarction by obstruction of blood flow in coronary arteries. (2) Hypoxic environment triggers cellular necrosis and the release of DAMPs. (3) Irritated endothelium expresses adhesion molecules and alert circulating innate immune cells. (4) Acute inflammatory response is initiated by neutrophil and monocyte recruitment, activation, and extravasation to the site of injury. (5) Pro- inflammatory environment triggers monocytes to macrophage M1 differentiation and activation. (6) Macrophages stimulate fibroblast proliferation and migration which further boost pro-inflammatory cytokines (i.e. IL-1, IL-6, and TNF-α), chemokines (i.e. MCP-1 and IL-8), release of proteinases (i.e. MMPs), and ECM degradation. Granulation phase: (7) Macrophage phagocytosis of necrotic debris and apoptotic neutrophils which triggers M2 macrophages activation. (8) M2 molecules (i.e. IL-10 and TGF-β) subside inflammation and stimulate fibroblast to myofibroblast differentiation. Myofibroblast becomes the major producer of ECM components and mediators of ECM deposition. Maturation phase: (9) Prolonged myofibroblast survival along with ECM crosslinking and fibrotic scar maturation and contraction [3].

D. Myocardial infarction (MI) and Type1 CRS development

Although the occurrence of type 1 CRS in the settings of MI is very common, its

underlying pathophysiology is poorly understood. Developed acute kidney injury in MI patients accounts for 25% to 40% of acute heart disease hospitalizations, increasing mortality rate substantially [4] [71, 72]. Accumulating pre-clinical and clinical evidence showed that both hypoperfusion and increased central venous pressure are crucial factors in type I CRS development [73]. At the onset of MI, MI-induced ventricular systolic dysfunction leads to a decrease in SV, cardiac output CO, and subsequent decrease in renal perfusion and glomerular filtration rate (GFR), eliciting systemic compensatory mechanisms [74]. Decreased arterial pressure to the kidneys as result of the compromised cardiac systolic function is met with an increased in central venous pressure and a decrease in GFR [75, 76]. Unlike physiological conditions, the compensatory mechanisms that are primarily mediated by SNS and RAAS activation are sustained in the presence of type I CRS, promoting subsequently adverse and progressive kidney damage [8, 77-79]. In addition to the SNS and RAAS activation, systemic inflammation and vasoactive compounds including endothelin, and NO along with prescribed diuretics can adversely affect renal perfusion independently of altered cardiac hemodynamics [80]. For instance, several experimental studies documented that type I CRS development highly correlates with enhanced monocytes activation and increased plasma pro-inflammatory cytokines (IL-1, IL-6, etc.) [81, 82]. Similarly, exogenous factors such as loop diuretic may contribute to kidney dysfunction by further fueling RAAS activation [83]. For example, Testani et al. reported that the use of high doses of loop diuretic was associated with a 5 fold increase in kidney dysfunction [84]. In Summary, SNS, RAAS, hemodynamics, vasoactive compounds, as well as the immune system regulate the bidirectional

interrelationship between the heart and the kidneys [80]. Any imbalance in these complex systems such as the systemic pathological response mediated by MI can aggravate cardiac and renal damage and constitute the basis of type I CRS development.

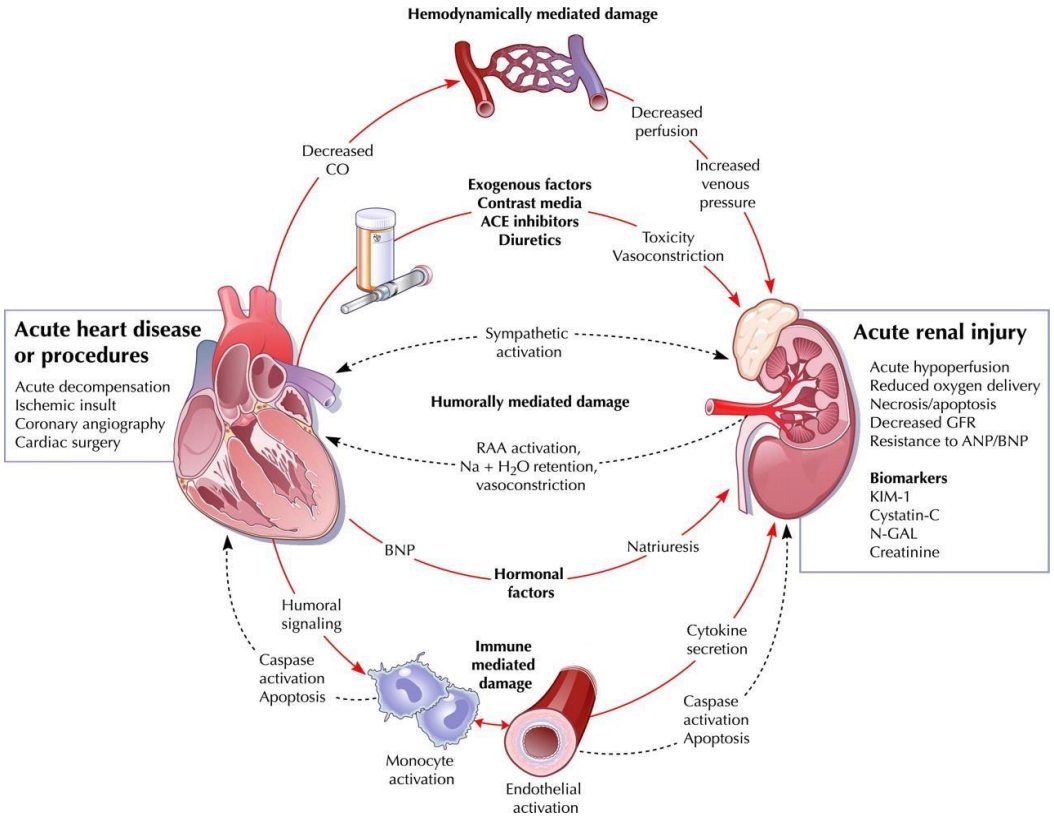

Figure 3 Type 1 Cardio-renal syndrome (CRS)

Pathophysiologic interactions between heart and kidney in type 1 or "acute CRS" (abrupt worsening of cardiac function; eg, acute myocardial infarction, acute cardiogenic shock or acute decompensation of chronic heart failure) leading to kidney injury. Abbreviations: ACE, angiotensin-converting enzyme; ANP, atrial natriuretic peptide; BNP, B-type natriuretic peptide; CO, cardiac output; GFR, glomerular filtration rate; H2O, water; KIM, kidney injury molecule; Na, sodium; N-GAL, neutrophil gelatinase- associated lipocalin; RAA, renin angiotensin aldosterone. Reproduced from Ronco et al27 with permission of Elsevier [2]

E. Diagnosis

Multiple biomarkers of tubular kidney injury and glomerular integrity including neutrophil gelatinase associated lipocalin, kidney injury molecule 1, and cystatin C are currently used in diagnosis of type I CRS.

1. Neutrophil gelatinase associated lipocalin (NGAL)

NGAL is a small protein located in neutrophils and it is freely filtered in glomerulus and completely reabsorbed in proximal convoluted tubules (PCTs). In the settings of kidney insult and within 24-48 hours following PCT injury, NGAL level is significantly elevated in both serum and urine (normal < 20ng/ml) [85, 86].

2. Kidney injury molecule 1 (KIM 1)

KIM-1 is tightly linked to the severity of kidney damage and peaking within 24 hours following PCT injury in the urine (normal < 200 ng/gCr). Unlike normal conditions, KIM 1 is expressed in regenerating PCT cells, promoting phagocytosis of apoptotic cells in the kidneys [87, 88].

3. Cystatin C

Cystatin C is produced in nucleated cells, freely filtered in glomerulus but not secreted in PCTs, and it is dramatically increased in plasma in kidney disease with reduced GFR. This marker is not influenced by muscle mass and thus it is better than serum creatinine with

respect to measured GFR [89, 90].

4. Creatinine

Creatinine is the end product of muscle creatine metabolism, freely filtered in glomerulus but not reabsorbed in PCT [91]. A significant amount of creatinine is secreted from PCTs into urine, thus this marker is highly influenced by variation in tubular secretion [92]. Additionally, sex, age, muscle mass are important modifiable factors that limit the accurate measurement of creatinine level in both plasma and urine [93]. Creatinine clearance is used to assess kidney function and to monitor kidney disease development (normal 110-150 ml/min in men, 100-130 ml/min in women) [94].

F. The Impact of CS On the Cardio-Renal System

Accumulating epidemiological studies linked CS to CVD development and prognosis. CS induces cardiac remodeling through four major interchangeable but overlapping mechanisms: ROS production, inflammation, apoptosis, and metabolic impairment.

1. Functional and Structural Mechanisms of CS-Induced Heart Damage

Multiple preclinical and clinical studies defined CS as a risk factor for adverse cardiac remodeling. In pathological response, CS-induced molecular and cellular changes in the heart can lead to structural damage such as ventricular hypertrophy/ dilatation, resulting in impaired LV systolic and diastolic function [17]. Two pathological mechanisms are involved in adverse cardiac hemodynamic changes following chronic CS: direct and indirect actions. Direct

actions of CS on cardiac muscle including necrosis, fibrosis, myocardial ischemia, and coronary vasoconstriction, leading to metabolic and morphological changes in the heart also known as smoke cardiomyopathy [17]. Indirect actions of CS are mediated through fueling other comorbidities and CHD risk factors such as hypertension, dyslipidemia, and inflammatory reactions [3] [58]. CS-induced adverse cardiac remodeling is well documented in multiple experimental studies. For instance, a significant increase in left ventricle end systolic diameter (LVESD) and left ventricle end diastolic diameter (LVEDD) were observed in a rat model exposed to 5 weeks of cigarette smoking [95]. Moreover, Talukder et al demonstrated that 32 weeks CS-exposed mice showed systolic and diastolic dysfunction in the LV of the heart [96]. Gvozdjakova et al. were the first to introduce the term smoke cardiomyopathy by referring to morphological alterations in the rabbit myocardium following chronic CS exposure and in the absence of comorbidities [97].

2. Molecular Mechanism of CS-induced Heart Damage

a. CS induced cardiac oxidative stress

Excessive ROS generation in response to CS promotes cardiac damage by inducing DNA denaturation, pro-inflammatory cytokines production, and lipid peroxidation [98]. These molecular and cellular changes can result in structural and functional alterations in the left ventricle of the heart. Duarte et al. demonstrated that CS accelerates cardiac remodeling post MI with increased GSSG and decreased GSH, GSH/GSSG ratio in both the heart and the liver. Eventually, GSH/GSSG imbalance causes an impaired anti-oxidant mechanism and enhanced systemic oxidant effect of CS on the heart [99]. Additionally, 8 weeks of CS-exposed animal

model revealed that CS induces lipotoxicity, mitochondrial dysfunction, and ROS production, therefore increasing cardiotoxicity [100].

b. CS induced cardiac inflammation

Several pre-clinical and clinical studies documented that increased inflammatory response in cardiac tissues is highly correlated with CS exposure [101, 102]. CS induced ROS production is involved in the inflammatory reactions by activating several pathways including NF-kβ, therefore promoting the production of pro-inflammatory cytokines such as IL-8 and TNF-a [103, 104]. Walter et al. reported that CS induces IL-8 production from infiltrating macrophages and monocytes [105]. Additionally, a 4 months CS-exposed rat model study showed an upregulation in pro-inflammatory cytokines such as IL-1β, TNF-a, and IL-6 while downregulating anti-inflammatory cytokines including IL-10 and TGF-β, subsequently accelerating adverse cardiac remodeling [106].

c. CS induced cardiac apoptosis

Apoptosis or "programmed cell death" is a crucial factor to maintain the health of organisms by promoting cell's turnover to replace malfunctioning cells [107]. Cardiac apoptosis is tightly correlated with increased ROS production and pro-inflammatory cytokines upregulation following CS exposure [100, 108, 109]. Das et al. demonstrated that CS induces extrinsic (caspase 8, TNF-α upregulation) and intrinsic (caspase 9, cytochrome c, and BAX/BCL2) apoptotic pathways in the myocardium [108]. Additionally, in a rat model study, CS-induced adverse cardiac remodeling through the activation of P38 and JNK of MAPK

signaling pathways [109]. Moreover, CS inhibits PI3K/AKT pathways resulting in increased apoptosis in the heart [17].

d. CS-induced metabolic impairment

Following CS exposure, cellular metabolic impairments were shown to accelerate ROS production, resulting in increased oxidative damage and subsequent inflammatory response [17]. Under physiological conditions, low ROS levels regulate multiple intracellular processes [110]. In contrast, excessive ROS generation alters mitochondria protein synthesis thus attenuating mitochondrial redox and ATP production levels, heightening subsequently cellular dysfunction and death [111]. In addition to their importance in regulating cell signaling and apoptosis, mitochondria regulates energy production in cardiovascular cells [112]. Pre-clinical studies indicated that CS increased mitochondrial permeability transition pore opening and oxidative stress, and decreased oxidative phosphorylation rate [113]. Gvozdjakova et al. reported that 3 weeks CS- exposed rabbits developed mitochondrial dysfunction via a significant decrease in oxidative phosphorylation, mito-respiration, and Q10 levels [97, 113].

3. Functional and Structural Mechanisms of CS-Induced Kidneys Damage

Heavy smoking is defined as a pivotal risk factor for kidney disease development. Experimental and clinical studies have postulated that CS causes multiple structural and functional deformities in the kidneys [114]. For instance, smokers are more prone to develop albuminuria, which is the early biomarker of kidney damage, when compared to non-smokers [115]. Hallan S.I. et al. reported that smokers are more likely to develop hypertension due to

increase in renin release from juxtaglomerular cells of the kidneys followed by angiotensin II production, a well-known potent vasoconstrictor [116]. Nicotine itself is known to aggravate kidney dysfunction by activating SNS (and renin and Ang II subsequently), resulting in renal vasoconstriction followed by a decline in renal blood flow and kidney perfusion [117]. Similarly, multiple pre-clinical studies highlighted the deleterious effects of chronic CS exposure on renal vasculature, including endothelial cell dysfunction, reduced vasodilatation, and decreased glomerular filtration rate (GFR) [118, 119]. In addition to CS-induced functional abnormalities, structural deformities following CS exposure have been also reported. For example, dilatation and atrophy in tubular basement membrane, and tubule interstitial fibrosis are well documented in a rat model of cigarette smoke exposure [120]. Along the same line, another experimental study elucidated that CS causes thickening in glomerular basement membrane. This alteration in glomerular structure results in kidney functional impairment such as reduced GFR and increased albuminuria [121]. Additionally, an in-vitro study indicated that CS leads to a decreased phagocytic capacity of mesangial cells therefore increasing catabolize materials accumulation in in glomerular capillary walls and further promoting kidney dysfunction [122].

4. Molecular Mechanisms of CS-Induced Kidney Damage

The adverse effects of CS on kidneys can be classified into four interchangeable mechanisms: ROS production, inflammation, fibrosis, and apoptosis.

a. CS- induced renal oxidative stress

Sustained increase in ROS production along with impaired anti-oxidant capacity within the renal cell can lead to progressive kidney damage [123]. Under physiological conditions, ROS production occurs in the course of oxygen metabolism and plays an essential biological role in the regulation of apoptosis, cell growth, and cell signaling transduction [124]. However, it is noteworthy to mention that CS is a well-known source of exogenous ROS and contains chemicals and irritants including free radical and oxidative gases that not only stimulate endogenous ROS production but also impair ROS anti-oxidant mechanisms [108, 125]. The impairment of the antioxidant defense mechanism caused by CS exposure can initiate or exacerbate molecular injury, such as DNA strand breaks and protein denaturation. These molecular changes can lead to renal fibrosis, apoptosis, necrosis, inflammatory reactions, and subsequently, structural and functional damage to the kidneys [123]. Gaurav et al. reported that 100 Nm nicotine stimulates NADPH oxidase-induced ROS production, promoting thereafter ERK1/ERK2 phosphorylation, subsequently increasing mesangial cells proliferation and fibronectin production in the kidneys [56].

b. CS-induced renal Inflammation

Irrespective of the underlying mechanism, inflammation increases mortality and morbidity rates in AKI [126]. A mouse model study reported that CS exposure induces renal TNF-α and IL-6 production, accelerating thereafter tubules and glomeruli damage [127, 128]. Michael E. Hall et al. showed a positive correlation between CS and increased CRP level, suggesting that CS-induced inflammation may contribute to kidney damage [129].

Additionally, an experimental study reported that CS increases Cystatin C level in plasma. Of note, Cystatin C is associated with decreased GFR and increased inflammation and is attributed to acute kidney injury development [130]. Once kidney insult is established, intrinsic and activated tubular renal cells express chemoattractants including adhesion molecules and chemokines, resulting in an influx of inflammatory cells such as leukocytes and macrophages into the tubulointerstitium [131]. Infiltrating macrophages contribute to the progression of kidney dysfunction through the production of proteolytic enzymes, inflammatory cytokines, ROS, and fibrogenic growth factors [132]. The trafficking of immune cells and cytokines fuel the production of profibrotic and proinflammatory factors, subsequently promoting myofibroblast differentiation, fibroblast proliferation, matrix secretion, and tubular atrophy [126, 132].

c. CS-induced renal fibrosis

CS-induced fibrosis highly correlates with kidney disease development [133]. In a 5/6 nephrectomy CKD rat model, the administration of nicotine induces a significant increase in the expression of TGF-β, and collagen, which are a well- known mediators of fibrosis [134]. Additionally, Arany et al. reported that 200μM nicotine promotes the effect of TGF-β1 on fibronectin and alpha smooth muscle actin (α-SMA) production in PCTs, accelerating thereafter fibrosis in the kidneys [135]. Yokoi et al. and Jensen et al. demonstrated that CS induces up-regulation of connective tissue growth factor (CTGF), a fibrogenic factor that triggers matrix protein synthesis and myofibroblast proliferation [136, 137]. These findings elucidated the important and direct role of CS-induced kidney damage [138]. Of note, the

progression of fibrosis extends over four phases: priming, activation, execution, and progression. The priming phase consists of two main events; the inflammation and the colonization of myofibroblasts. Kidney insult establishes a pro-inflammatory environment, therefore activating the infiltration of macrophages and monocytes to the site of injury [128, 138, 139]. Persistent inflammation leads to an accumulation of pro-fibrotic mediators followed by a phenotypic transition of fibroblasts to myofibroblast [133, 139]. The activation phase is characterized by a high rate of production of different growth factors and pro-inflammatory cytokines. This cascade of events induces ECM producing myofibroblast in preparation for fibrogenic events [138, 139]. The execution phase is characterized by an excessive generation of ECM in association with of myofibroblasts over-proliferation, a significant indicative of fibrosis [133, 138, 139]. The progression phase is characterized by a remarkable reduction in nephron numbers and thus GFR [138, 139].

d. CS-induced renal apoptosis

Disequilibrium and excessive apoptosis are significantly heightened in AKI. Soo wan kim et al. reported that nicotine induces apoptosis by changing the ratio of Bax/Bcl2. Bax is a pro-apoptotic biomarker that binds to the mitochondria membrane permeabilization enhancing cytochrome c release, thus eliciting renal apoptosis [140] [141]. Additionally, nicotine promotes apoptosis through increased ROS production, induced ERK1/2, JNK and P38 phosphorylation in human podocyte cells.[135, 142] [143].

G. CS and Gender Bias

Accumulating epidemiological studies reported that the ratio of female-to-male smoking prevalance in middle and low-income countries is on the rise. Although CS-induced adverse effects on the cardiovascular and renal systems is well established in males, little is relatively known about the impact of CS on the females systems as well as the gender discrepancies in type I cardio-renal syndrome (table 1). The prevalence of cardiovascular and kidney diseases in pre- menopausal women are less frequent than age-matched men, but picks up wih age to reach similar levels in the post-menopausal phase [144]. Sexual dimorphisms are potentially attributed to the protective role of endogenous estrogen E2 (17-β Ethinyl Estradiol). Pre-clinical and clinial studies suggested that E2 effects are primarily mediated by two types of receptors; ERα and ERβ. Lagranha et al. showed that E2 plays a cardioprotective role in premenopausal female rats following ischemia reperfusion I/R injury by decreasing infarct size and promoting cardiomyocyte contractility [145]. Additionally, Zhang et al. demonstrated that lower coronary blood flow, higher incidence of tachycardia, and increased infarct size were observed in the hearts of ErαKO mice compared to wild type mice [146]. Along the same line, the direct cardio-protective role of Erα was observed in MI induced-female mice by using Erα agonist (PPT), resulting in decreased infarct size and enhanced cardiac function [147]. Erβ receptors, on the other hand, exert indirect cardioprotective effects by lowering blood pressure and modulating the autonomic cardiac control [51]. Several experimental studies correlate E2 with improved kidney function. For instance, Kummer et al. reported that E2 exerts anti-apoptotic effects on podocyte cells through attenuating the opening of the mitochondrial permeability transition pore and decreasing the release of pro-

apoptotic biomarkers into cytosol [148]. Additionally, Seppi et al. elucidated that PCT renewal mechanism is cyclically regulated by female sex hormones, resulting in increased cell turnover, subsequently enhanced PCT repair capacity [149].

Experimental Model	Published Studies	Animal Model/Gender	Outcomes
MI	Yes	MI± transgenic (Tg-ERβ) female mice	ERβ inhibits myocardial fibrosis and promotes NO synthesis following MI [146]
	Yes	MI± transgenic male and female mice with cardiomyocyte specific overexpression of ERα (ERα-OE)	Enhanced angiogenesis and inhibited cardiac fibrosis were only observed in female (ERα-OE) mice [147]
MI + CS	N/A	N/A	N/A
AKI	Yes	Renal ischemia (RI) induced in male and female rats	Increased e-NOS activity, HIF-α expression, and enhanced antioxidant mechanism in RI-induced female compared to male rats [150]
	Yes	Renal Ischemia Reperfusion (RIR) induced in male and female rats ± single dose of E2 (500 μg/kg)	E2 treated groups demonstrated enhanced anti-oxidant and anti inflammatory defense mechanisms, and increased e-NOS activi in both genders [151]
		15 months old	

AKI+ CS	Yes	ovariectomized CS exposed female mice ±E2(25μg release pellet)	E2 mediated ER-α activation decreases CS induced TGF-β, SMAD3, and IGFR m-RNA expression [152]
Type I CRS	N/A	N/A	N/A
Type I CRS + CS	N/A	N/A	N/A

H. Thesis Rationale

CS is a major risk factor for CVDs and kidney dysfunction in both genders. WHO estimates more than 5 million deaths annually caused by direct CS exposure [153].

MI is on the rise in the Lebanese society and worldwide. According to WHO 31% of CVD- related death is due to coronary heart diseases mostly MI. (http://www.who.int/cardiovascular_diseases/en/).

MI is the leading cause of type I CRS development [154]. CS exacerbate MI induced kidney damage in male mice [155].

Numerous hemodynamic studies highlight the negative impact of CS on LV remodeling in males [156].

The incidence of cardiovascular diseases in pre-menopausal women is less frequent than age-matched men, but picks up wih age to reach similar levels in the post- menopausal phase [157].

The prevalence of kidney dysfunction through the cardio-renal interrelationship is less in females compared to age-matched males [144].

This is the first study to investigate the impact of CS on MI-induced renal damage in type I (CRS) between males and female mice. The findings of this study will have national and international awareness and scientific impact.

I. Thesis Hypothesis and Aims

Our understanding of kidney damage in type I cardio-renal syndrome following CS exposure is not well elucidated. Most of the studies focused on the impact of CS-induced kidney damage in males. To date, the exact mechanisms behind the impact of harmful CS compounds on MI induced kidney dysfunction through the cardio-renal interrelationship remain poorly understood and is the main focus of our study. Based on our rational supported by published evidence, we hypothesize that kidney damage post-CS exposure is worsened in both MI genders with female MI mice being more protected. This is the first study to assess the impact of CS on kidney damage in the presence of MI in females. The main Aim of this study is to investigate whether CS exposure causes worsened kidney damage in MI-male mice when compared to relative female mice.

CHAPTER II

MATERILAS AND METHODS

A. Study Input

Sixty, 5 months old C57Bl/6J, male and female mice were used to carry on the experiments proposed in the aim of this study. As detailed in figure 4, mice were divided into 2 groups: 30 males and 30 females. Each group was then divided into 3 subgroups: 10 controls, 10 MI and 10 MI+CS.

1. Study Design

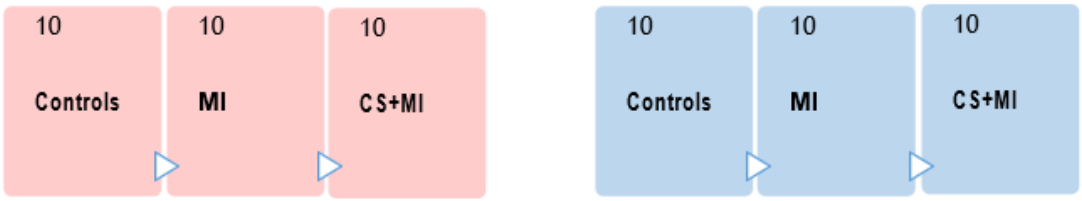

Figure 4 Study design

Baseline BP and baseline Echo were recorded. Mice were then enrolled in two weeks of CS exposure with BP and echo recorded at the end of week two, followed by MI induction. Mice were exposed to CS for another week post-M before sacrifice at the end of week 3.

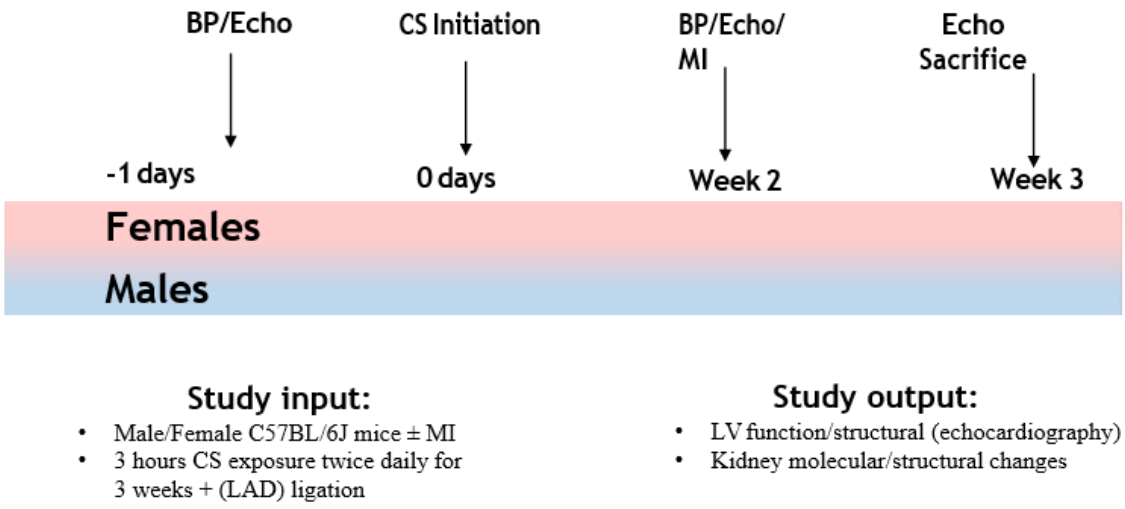

Figure 5 Study Design Timeline

B. Animal Use

According to the "Institutional Animal Care and Use Committee" (IACUC) guidelines, age matched male and female C57BL/6J mice were used in this study. In the animal care facility at AUB, 5 months old mice were maintained under pathogen free optimum conditions with 12 light/12dark hours cycle and were allowed to unlimited standard chow and water access. Animals were distributed according to the Study Design as detailed in the section above.

C. Hemodynamics and LV Function Assessment

1. Echocardiography

Echocardiography was performed according to the American Society of

Echocardiography guidelines using Vevo 2100™ High-Resolution Imaging System (Visual Sonics, Toronto, Canada). Briefly, general anesthesia was induced with isoflurane (1.5% in oxygen) inhalation. Rectal thermostat and warming plate were used in order to monitor and maintain body temperature at 37 Co. M-mode and B-mode echocardiography images were obtained in the parasternal long- and short-axis views by placing the transducer on the left thorax and directing ultrasound beam at the mid papillary muscle level. Continuous interface of the anterior and posterior walls was visualized and well defined before measurements. For all animals, mean calculations of ejection fraction (EF) and cardiac output (CO) were measured for three or more consecutive cardiac cycles at baseline, at the end of week 2, and right before sacrifice.

2. Blood Pressure in fully conscious mice

Blood pressure was measured using the tail cuff- method (CODA-2, Kent Scientific, Torrington, CT) under fully conscious conditions. This method allows real- time recording of tail blood flow, tail blood volume, heart rate, systolic BP, diastolic BP, and mean BP based on volume pressure recording (VPR) sensor technology. Mice were trained for 3 days by measuring BP daily. Each BP session consisted of 5 acclimatization cycles followed by 15 BP measurements. The average of mean BP, diastolic BP and systolic BP from each BP session and in each mouse was used

D. CS Exposure

(ONARES, CH Technologies, USA) nose only exposure apparatus was used to expose restrained and conscious C57BL/6J aged-matched male and female mice to mainstream

smoke. This apparatus has been extensively used to study smoking related disease This smoking machine includes a puffer generating puffs at a constant frequency of one puff/50 second, a volume 2 ml/puff and duration of 2.5 second/puff. 3R4F scientific cigarettes (University of Kentucky, Lexington, KY, USA) were used allowing a total particle matter (TPM) concentration of about 100 mg/ cm3/mouse/session, 9.4 mg tar, and 0.726 mg nicotine per cigarette. Mice received two 90-minutes sessions daily, 7days/week for 2 weeks before inducing MI, then one week after.

E. MI Induction

MI was induced by left anterior descending (LAD) coronary artery ligation. To eliminate any pre-existing co-morbidities that may complicate surgical outcomes, hemodynamic examinations including heart rate (HR), BP, body temperature, respiratory rate and body weight were performed. 15 min prior to MI, mice were given tramadol (0.05-0.1 mg/kg i.p.) to induce general anesthesia. To prevent hypothermia, the mouse was placed on a heating pad and anesthetized by using isoflurane (2-3% in oxygen) inhalation. Normal respiratory rate was maintained by performing orotracheal intubation by placing a needle into the trachea, connected to mini ventilator (Harvard Apparatus). After the animal's left thorax incised, LAD coronary artery, left ventricle, and left atria were exposed. MI was induced by LAD ligation with 7-0 polypropylene suture at 1-3mm underneath the left atrium appendage. To confirm MI and assess infarction size, 2,3,5-triphenyltetrazolium chloride TTC staining (Sigma-Aldrich) was used. Each left ventricle was sliced into base, midsection and apex. Both left ventricle slices and right ventricle were incubated with 1% TTC staining for 15 min at

37oC. The infarct size (appears in white) was measured by using Image j software (https://imagej.nih.gov/ij/) as a percentage (infarct size/risk area %) of the risk area (appears in red). Then the thorax was closed. Mice were monitored on a daily basis to ensure fully recovery.

F. Necropsy (Sacrifice Steps)

At the end of the experiment, mice were sacrificed as follow:

1. To perform anesthesia, all mice were exposed to isoflurane vapor (Forane®) diluted with O2.

2. 5 min prior sacrifice, heparin injections were given to mice to simplify blood collection.

3. 100 uL cardioplegic solution was injected in order to arrest the heart of mice at diastole phase of cardiac cycle.

4. Upon removal LV remote and infarcted areas were snap frozen in liquid nitrogen for RNA and protein extraction and mid sections were suspended in formalin-containing storage vials for histology analysis.

5. To assess cardiac hypertrophy, heart weight/tibia length ratio was used.

6. Kidneys were divided into two sections; right kidney and left kidney. For histopathology, right kidney was fixed in formalin and embedded in paraffin. Whereas, left kidney was snap frozen in liquid nitrogen for further molecular analysis.

G. Immunohistochemistry

1. Hematoxylin and Eosin (H& E) Staining

To highlight glomerular retraction for all experimental groups, H&E staining was used. Hematoxylin is a deep blue-purple stain with an affinity to acid, thus it stains nucleic acid. Whereas, Eosin has a pink color and stains protein nonspecifically. Briefly, kidney tissues were fixed in 10% formalin, dehydrated and then embedded in paraffin. 4 μm thickness kidney sections were deparaffinized, rehydrated, stained with H&E and then examined under light microscope.

2. Masson's Trichrome Staining

Masson's Trichrome staining is used to study collagen deposition and fibrosis. Dewaxing and hydration steps were done, then kidney tissues were soaked in Bouin solution at 56 Co for one hour, washed in running tap water, and rinsed in distilled water. After 10 min incubation with hematoxylin, a second washing step was done, and kidney tissues were then stained in biebrich scarlet acid fuchsin for 10 min. kidney sections were washed and differentiated in phosphomolybdic- phosphotungstic acid solution for 10 min, transferred to aniline blue solution, stained for 5 minutes and observed using light microscopy. Fibrosis was measured using Image J software (https://imagej.nih.gov/ij/).

3. Periodic Acid Schiff (PAS) Staining

Control, MI, and MI+CS groups were stained with PAS to detect PCT dilatation by using Image J software (https://imagej.nih.gov/ij/). PAS stains carbohydrate and polysaccharides including glycogen, resulting in a pink color. Dewaxing and hydration steps

were performed to the paraffin embedded kidneys. Kidney tissues were incubated with 0.5% PAS staining for 10 minutes, then with the Schiff reagent for 10-20 minutes and washed for 5 minutes. Dehydration with increased percentage of ethanol (75, 95% and 100%) were done. Finally, slides were mounted and observed under light microscope after cleaning with xylol.

H. Molecular Analysis

1. Dihydroethidium (DHE) Staining

DHE staining (Calbiochem, Darmstadt, Germany) was used to assess the levels of glomeruli reactive oxygen species (ROS). Briefly, unstained slides were incubated with 10 µM DHE in a humidified chamber under dark condition for 45 min at room temperature. Laser Scanning Fluorescent Microscope (Zeiss Axio) was used to acquire images for kidney tissues under 20x magnification.

2. Terminal deoxynucleotidyl transferase dUTP nick end labeling (TUNEL)

TUNEL assay is used to assess DNA fragmentation. Kidney tissues were mounted on slides, dewaxed and rehydrated. DNA fragmentation detection kit was used to perform TUNEL staining as described by manufacturer's instructions. On the slides, glomeruli with green nuclear labeling were considered as TUNEL positive. DNA fragmentation was evaluated by using Laser Scanning Fluorescent Microscope (Zeiss Axio) under 20x magnification.

3. Protein Extraction and Western Blots

Control and experimental snap frozen kidneys were crushed under liquid nitrogen.

Extraction buffer composed of 100 Mm dithiothreiol, 1% sodium dodecyl sulphate (SDS), 0.9% NACL, and 80 Mm Tris hydrochloride (PH 6.8) was used to kidney homogenization. The samples were heated for 10 min at 95oC left overnight on rocking shaker at 4oC.

150 μg of kidney tissues were loaded into the wells of 15% sodium dodecyl sulphate polyacrylamide gel electrophoresis (SDS-PAGE). Proteins were then run until the dye reached the bottom of the gel and transferred onto a nitrocellulose membrane at 100 volts, for 1 hour, at 4 C. Blocking of the membrane was done by using 5% free-fat milk dissolved in TBST 0.1% (Tris buffer saline with 0.1% Tween 20) , at room temperature for 2 hours. Afterward, membranes were incubated with a dilution of polyclonal primary antibodies in 0.1% TBST overnight at 4 C. The membranes were then washed with 0.02% TBST (4*5min) and incubated with 1:40000 biotin- conjugated secondary antibody in 0.1% TBST for one hour at room temperature. Afterwards, membranes were washed and incubated in 1/200000 HRP-conjugated streptavidin for 30 min. After washing with 0.02% TBST (2*5min) and TBS (2*5min), sufficient volume of ECL chemiluminescence kit (Biorad) was added to the membranes to be then visualized using chemidoc MP imaging system- Biorad Protein expression level was normalized to total protein [158], and analyzed using image J software (https://imagej.nih.gov/ij/)

Primary antibody	Dilution/Concentration
Anti IL-1β (Abcam)	1/500
Anti IL-4 (Abcam)	1/1000
Anti IL-10 (Abcam)	1/1000
Anti IL-13(Abcam)	1/500
Anti pro-caspase 3(Abcam)	1/500
Anti-α-SMA(Abcam)	1/200

Table 2:
List of used antibodies

4. RNA Extraction and Real Time q-PCR

Snap frozen kidney tissues were ground in liquid nitrogen by a mortar and pestle then total RNA was extracted using Trizol according to manufacturer's instructions (Thermo Fisher Scientific, Grand Island, NY,USA). NanoDrop® ND-1000 UV-Vis Spectrophotometer was used to quantify RNA. RNA purity was assessed using the absorbance ratio of 260 to 280 nm, where a value of 1.8-2.0 indicated good quality RNA. Real time q- PCR was used to quantify differences in m RNA expression. During RT step, cDNA was synthesized from 1µg RNA, using Revert Aid 1st Strand cDNA synthesis kit (Thermo, USA), followed by real time PCR analysis in a CFX96 real-time PCR system (Bio-Rad, Germany). Then the synthesized cDNA was loaded in duplicate with 0.05 µM of the forward and reverse primers of the gene of interest and mixed with SYBR® Green for qPCR steps. Gene expression was monitored using SYBR® Green PCR Master Mix (Bio-Rad, Hercules, CA, USA) to quantify the expression of

MMP8, MMP13, CTGF, α-SMA, NMRK1, NAMPT, SIRT1, SIRT3, and PARP-1. GAPDH was used to normalize gene expression between the different samples. To check for non-specific amplification, no-template control (water without DNA) was used. Normalized fold expression relative to the control was calculated and plotted by Biorad CFX-manager to compare differential gene expression.

Primer	Forward	Reverse
MMP8	CACACTCCGTGGGGAGATTT	GCCTGAAGACCGTTGGGTAG
MMP13	AGAAGTGTGACCCAGCCCTA	GGTCACGGGATGGATGTTCA
CTGF	ACCCAACTATGATGCGAGCC	GGTAACTCGGGTGGAGATGC
a-SMA	CAGCGGGCATCCACGAAA	GGCCCAGCTTCGTCGTATT
NAMPT	ACCAGCGGGGAACTTTGTTA	ACATAACAACCCGGCCACAT
NMRK1	CTTGAAGCTTGCTCTGCGAC	GTGTCGTCTTCCCTCCGTTT
SIRT1	CGGCTACCGAGGTCCATATAC	ACAATCTGCCACAGCGTCAT

Table 3:
List of primers

5. Immunofluorescence (IF)

IF was used to assess the protein expression level of α-SMA in kidney tissues. Kidney slides were placed in an antigen retrieval buffer for 15 min at 95 C°, then washed with TBS two times for 5 min each. 10% NGS was used to block non- specific binding of α-SMA antibody for 2 hours. Kidney tissues were then incubated with a dilution of α-SMA antibody in TBS (1:200) overnight at 4 C°, followed by two washes with TBS for 5 min each. Afterward, slides were incubated with a dilution of secondary antibody (FITC) in TBS (1:100) for 1 hours, followed by 2 washes with TBS, 5 min each. α-SMA protein expression level was then quantified using Laser Scanning Fluorescent Microscope (Zeiss Axio) under 20x

magnification.

I. NAD extraction and Quantification

Kidney tissues were extracted using 75% ethanol, 25% HEPES 10 mM pH7.1, buffer (20 µl/mg of tissue) and diluted in water to a final volume of 25 µl to reach a concentration within the standard curve. Extracts were then added to 100 µL of reaction buffer (600 mM ethanol, 0.5 mM 3-(4.5dimethylthiazol-2-yl)-2.5- diphenyltetrazolium bromide (MTT), 2 mM phenazine ethosulfate (PES), 120 mM Bicine (pH7.8), yeast alcohol dehydrogenase (SIGMA A3263 > 300 u/mg) 0.05mg/ml. Kinetics of the reaction (OD at 550nm, every 30 seconds for 20 minutes) was followed on LB 942 Multimode Reader. NAD was quantified in duplicates for each sample by comparison to a range of standard NAD concentration using linear regression curve equation method between NAD standard concentrations and the slope of the reaction.

J. Statistical Analysis

Results are expressed as raw data or as the Mean ± SEM. TUKEY Statistical comparisons were performed using two-way analysis (ANOVA) with appropriate post-hoc test to determine statistical significance. The p value was determined and values for $p<0.05$ (*) were considered significant. Microsoft Excel and GraphPad software were used to perform statistical analysis.

CHAPTER III

RESULTS

A. Hemodynamics and LV function assessment

1. Female and male MI mice presented no change in SBP following 2 weeks of CS

Following 2 week of CS exposure, no marked increase in SBP in both genders was noted. Therefore, at the onset of MI, BP measurements between male and female mice were not significantly different and could not account for any observed differences in cardiac remodeling between genders post-MI.

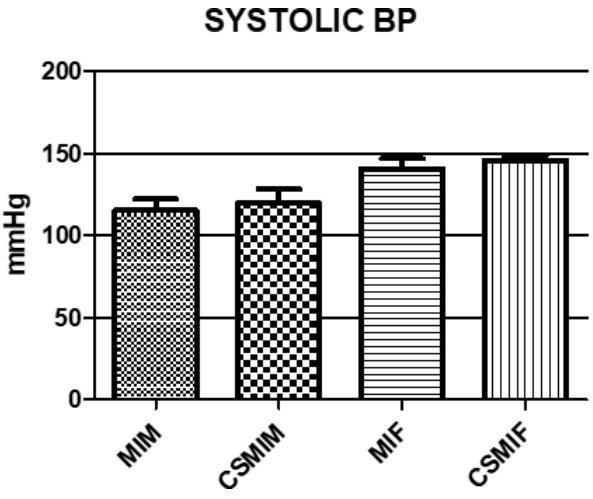

Figure 6 Comparison of SBP in non-CS exposed and CS-exposed MI male and female mice

before undergoing MI, showing no change in all groups. MI: Myocardial infarction; MIF: MI female mice; CSMIF: Smoking MI female mice; MIM: MI male mice; CSMIM: Smoking MI male mice. Values are represented as mean ± s.e.m.; Two-Way-Anova statistical analysis.

2. Significant decrease in EF in CS-exposed MI male mice when compared to CS exposed MI female mice

EF was significantly decreased in non and CS-exposed MI male and female mice compared to control groups. Of note, a marked decrease in EF was observed in MI male mice following CS exposure when compared to the relative female subjects, suggesting a worsened cardiac remodeling post CS exposure in MI male mice.

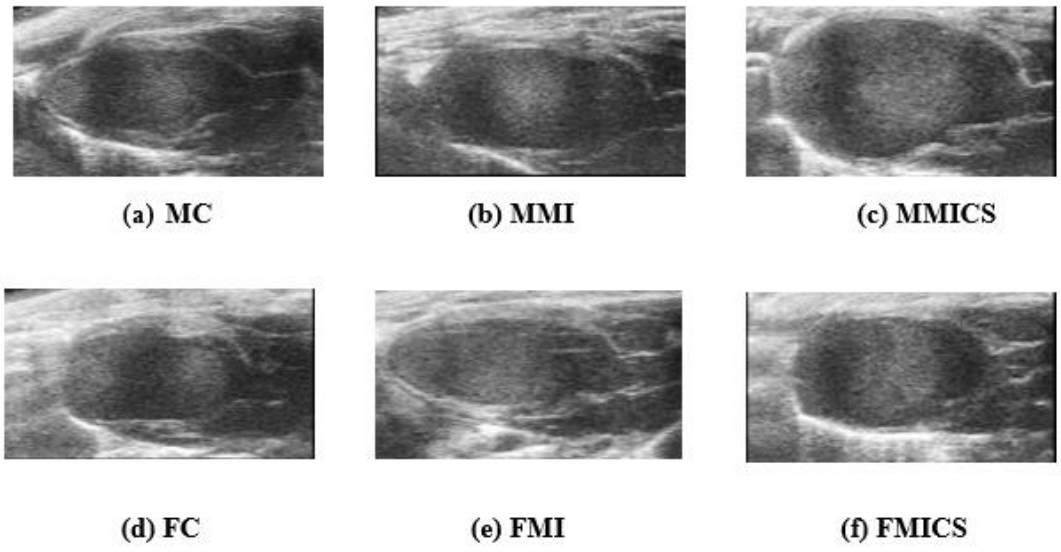

(a) MC **(b) MMI** **(c) MMICS**

(d) FC **(e) FMI** **(f) FMICS**

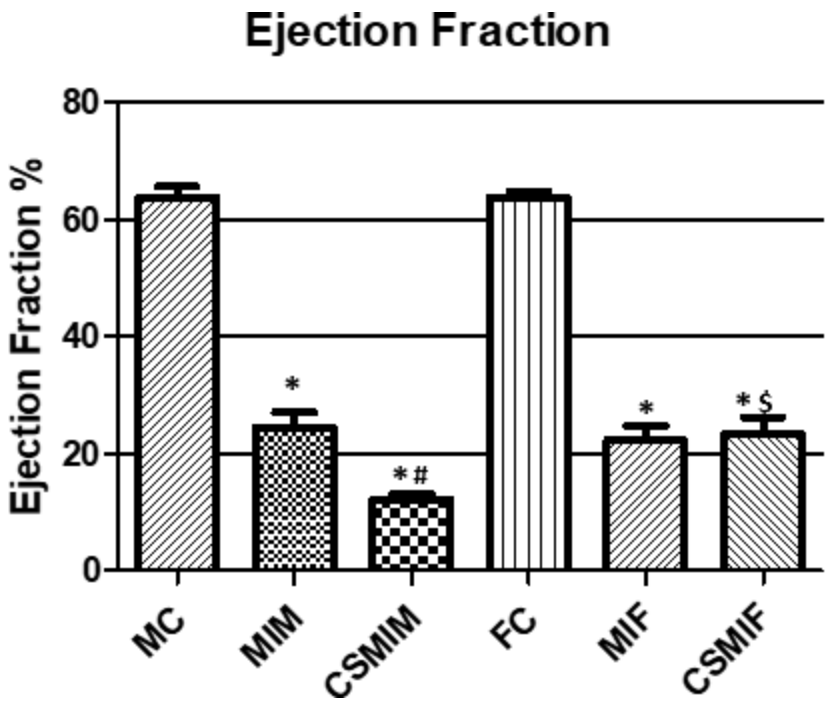

Figure 7 Typical B-mode images of parasternal long-axis view

(a) representative Control male mice group; (b) representative non-CS exposed MI male mice group; (c) representative CS-exposed MI male mice group; (d) representative control female mice; (e) representative non-CS exposed MI female mice group; and (f) representative CS-exposed MI female mice group. Ejection fraction is also calculated for each group showing effects of CS exposure on cardiac function after MI and MI+CS. EF was significantly decreased in non and CS- exposed male and female mice. Of note: the decrease in EF was markedly heightened in CS-exposed MI male mice when compared to their relative female group. C: Control; Myocardial infarction; CS: Cigarette smoking. (N=10); represented as; Values are represented as mean ± s.e.m.; Two-Way-Anova statistical analysis; p value<0.05

3. Significant decrease in Cardiac Output (CO) in CS-exposed MI compared to non CS-exposed MI male mice

A significant decrease in CO in CS-exposed MI compared to non CS-exposed MI male mice was observed. In female mice, on the other hand, no marked depression in CO following CS exposure was noticed. These findings suggest a worsened systolic cardiac function following CS exposure only in male groups.

Figure 8 Cardiac Output (CO) variation

A significant decrease in CO was observed in non CS- exposed MI male and female mice when compared to their controls. Of note, CO was markedly decreased following CS in MI male mice. However; no significant change was noted in CS-exposed MI female mice. C: Control; MI: myocardial infarction; CS: Cigarette smoking; *: Significance between MI and Ctrl; #: Significance between MI+CS and MI; One Way Anova (N=10); P value< 0.05

B. Histological analysis of the kidneys

1. Glomerular retraction was significantly increased in CS-exposed MI male compared to CS-exposed MI female mice

We examined glomerular retraction in control, MI and MI+CS groups (n=8/group) in both genders using H&E staining. Figure 10 shows that glomerular retraction was strongly heightened in non CS-exposed and CS-exposed MI male and female mice compared to their relative subjects. Of note, glomerular retraction was significantly increased in MI males following CS exposure when compared to the relative female subjects.

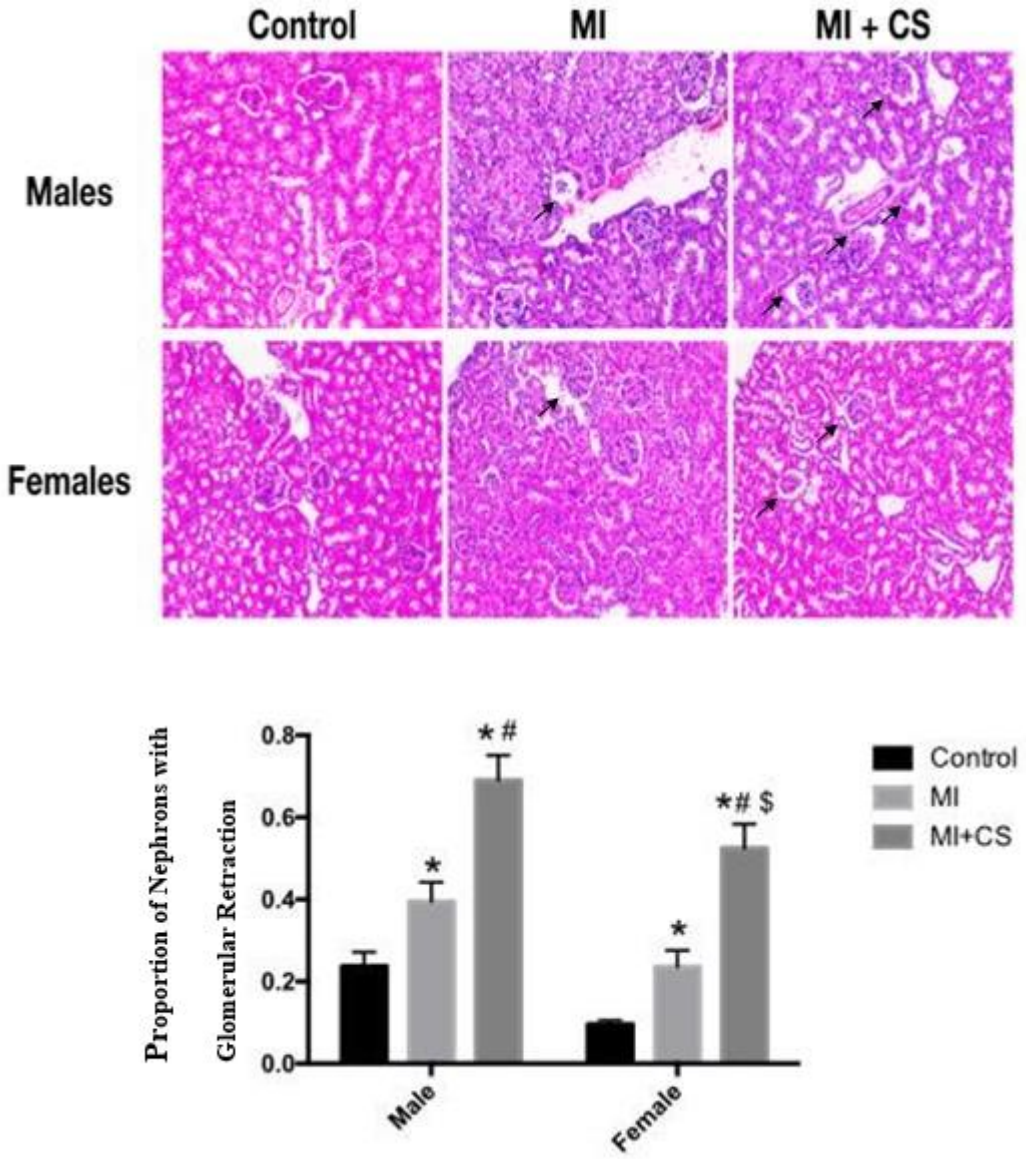

Figure 9 Effect of CS and MI on kidney histopathology, using H&E staining

Non CS- exposed MI male and female mice showed a significant increase in glomerular retraction compared to baseline. A significant increase in CS- exposed MI to non CS-exposed MI in both genders was also noted. Ctrl: Control; MI: Myocardial infarction; CS: Chronic cigarette smoking; *: Significance between MI and Ctrl; #: Significance between MI+CS and MI; $: Significance between male and female mice; (n=8); Values are represented as mean ± s.e.m.; Two-Way-Anova statistical analysis; p value<0.05

2. ***Proximal Convoluted Tubule (PCTs) dilatation was heightened in CS- exposed MI males when compared to relative females group***

PCT dilatation was assessed in all experimental groups (n=5/group) in both genders using PAS staining. Figure 11 shows a significant increase in PCT dilatation in CS-exposed MI male mice compared to control and non-CS exposed MI male groups. Of interest, no significant change in PCT dilatation was observed between all female groups, however, all female groups had a significantly less PCT dilatation than the relative male groups.

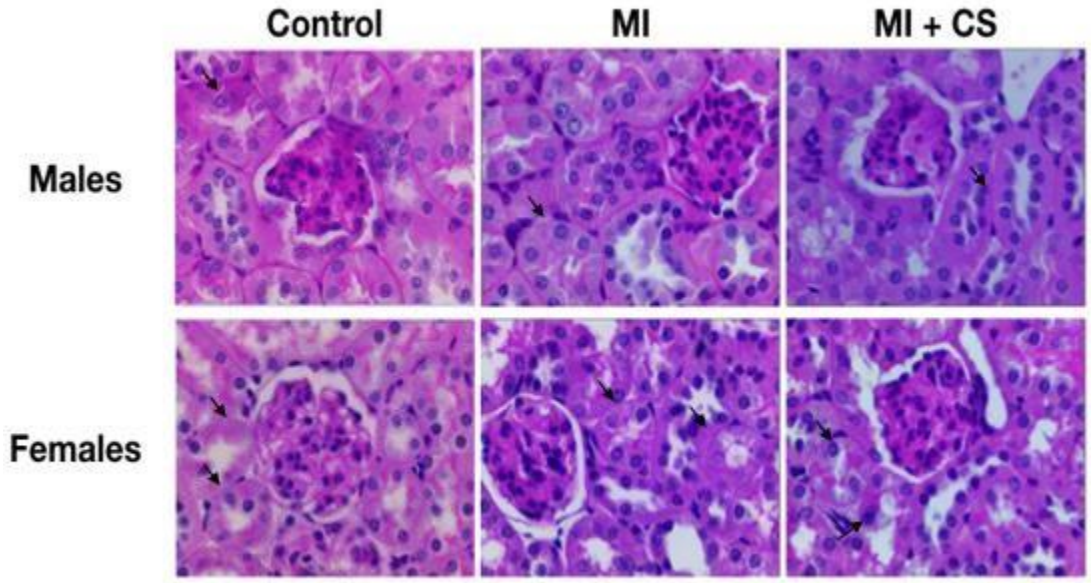

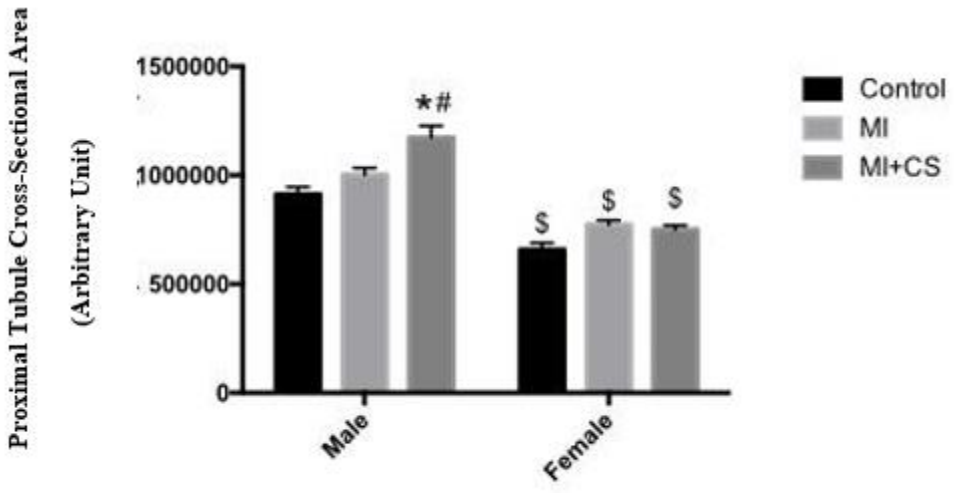

Figure 10 Effect of MI and CS+MI on kidney histopathology: PAS staining

showed Significant dilatation in Proximal Convoluted Tubules (PCTs) in CS-exposed MI males compared to the relative female subjects. Ctrl: Control; MI: Myocardial infarction; CS: Chronic cigarette smoking; *: Significance between MI and Ctrl; #: Significance between MI+CS and MI; $: Significance between male and female mice; (n=5); Values are represented as mean ± s.e.m.; Two-Way-Anova statistical analysis; P value <0.05

3. Increased fibrosis in non CS-exposed and CS-exposed MI male compared to the relative female mice

Interstitial fibrosis was assessed in control, MI and MI+CS male and female mice (n=5/group) using Masson's Trichrome staining. Figure 12 shows that both genders showed a significant increase in interstitial fibrosis following MI and CS exposure when compared to their relative controls. Importantly, interstitial fibrosis was significantly heightened in non CS-exposed and CS-exposed MI males when compared to the relative female groups.

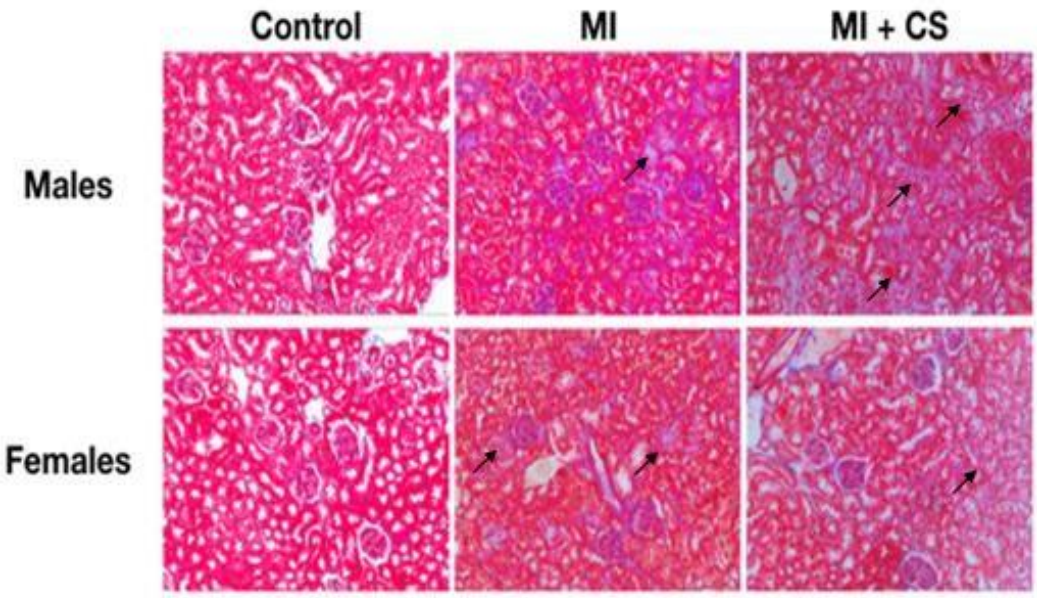

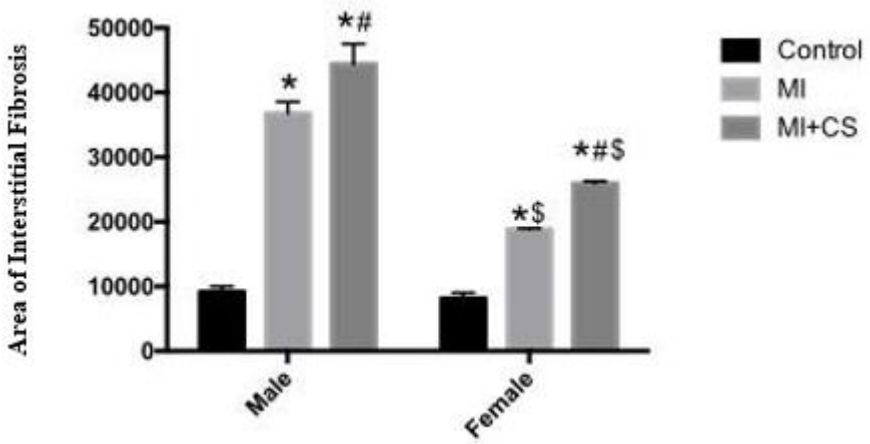

Figure 11 Effect of MI and MI+CS on kidney histopathology: Masson's staining

showed significantly increased interstitial fibrosis in both non CS- exposed and CS- exposed MI male and female mice compared to controls and non CS-exposed MI groups respectively. Ctrl: Control; MI: Myocardial infarction; CS: Chronic cigarette smoking; *: Significance between MI and Ctrl; #: Significance between MI+CS and MI; $: Significance between male and female mice; (n=5); Values

are represented as mean ± s.e.m.; Two-Way-Anova statistical analysis; p value< 0.05

C. Molecular analysis of the kidneys

1. No gender based differences in glomeruli ROS production between male and female mice was observed in CS effect on MI induced kidney damage

Glomeruli ROS production was assessed using DHE staining in all mice groups (n=3/group). Figure 13 shows that glomeruli ROS production was significantly heightened in non CS and CS-exposed MI male and female mice compared to their relative subjects. However, no gender differences in ROS production was noticed.

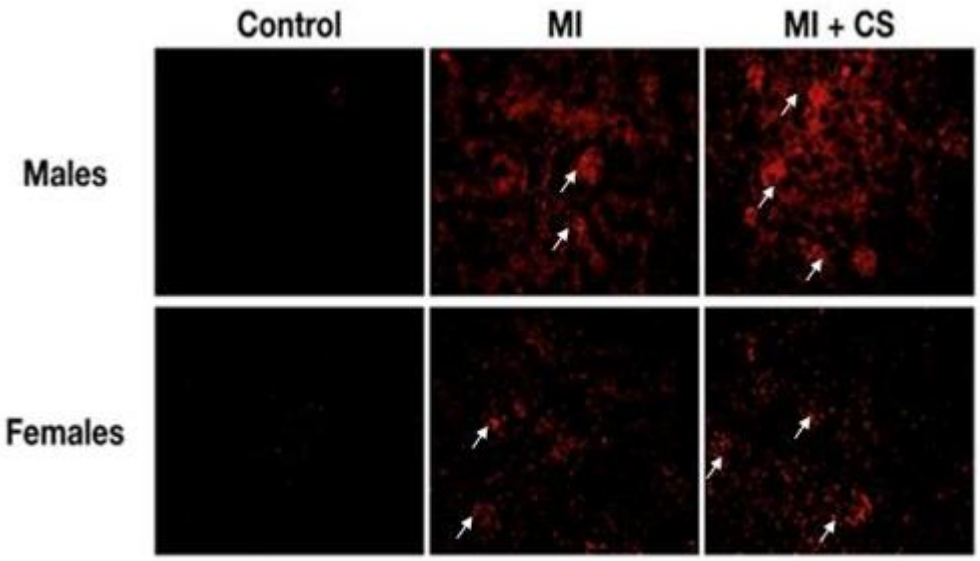

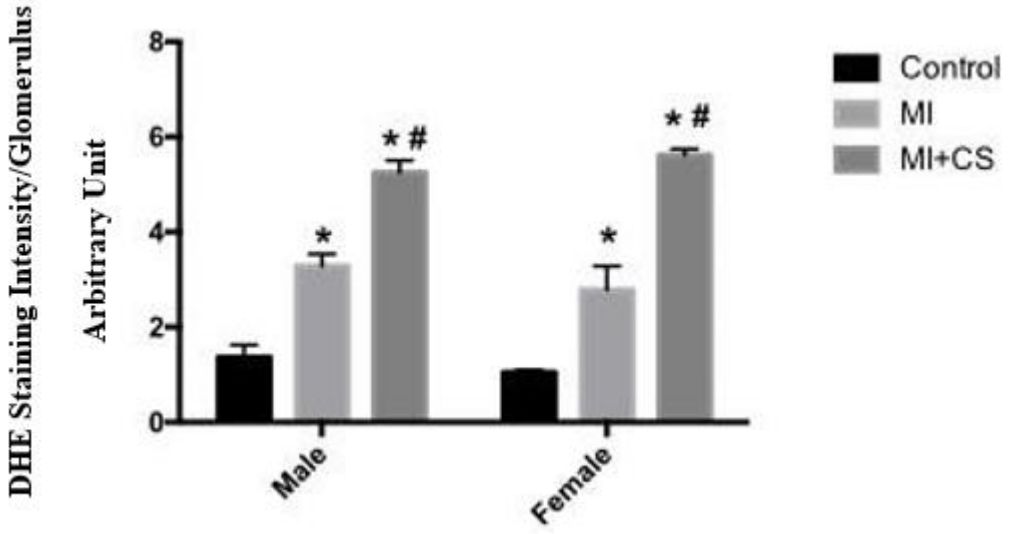

Figure 12 Effect of MI and MI+CS on glomeruli ROS production

in kidney tissues using DHE staining showed significant increase in glomeruli ROS generation in non CS-exposed and CS-exposed MI compered to Ctrl and non- CS exposed MI groups respectively in both genders. Ctrl: Control; MI: Myocardial infarction; CS: Cigarette smoking; *: Significance between MI and Ctrl; #: Significance between MI+CS and MI; (n=3); Values are represented as mean ± s.e.m.; Two-Way-Anova statistical analysis; P value<0.05

2. Glomeruli DNA fragmentation was markedly increased in non CS-exposed MI male when compared to non CS-exposed MI female mice

Glomeruli DNA fragmentation was assessed in all experimental groups using TUNEL assay: Figure 14 showes a significant increase in DNA fragmentation in male mice following MI and MI+CS compared to control. DNA fragmentation in female mice was markedly heightened in non-CS and CS-exposed MI groups compared to control and non CS-exposed mice respectively. Importantly, higher DNA damage was observed in non CS-exposed MI males when compared to non CS-exposed MI females.

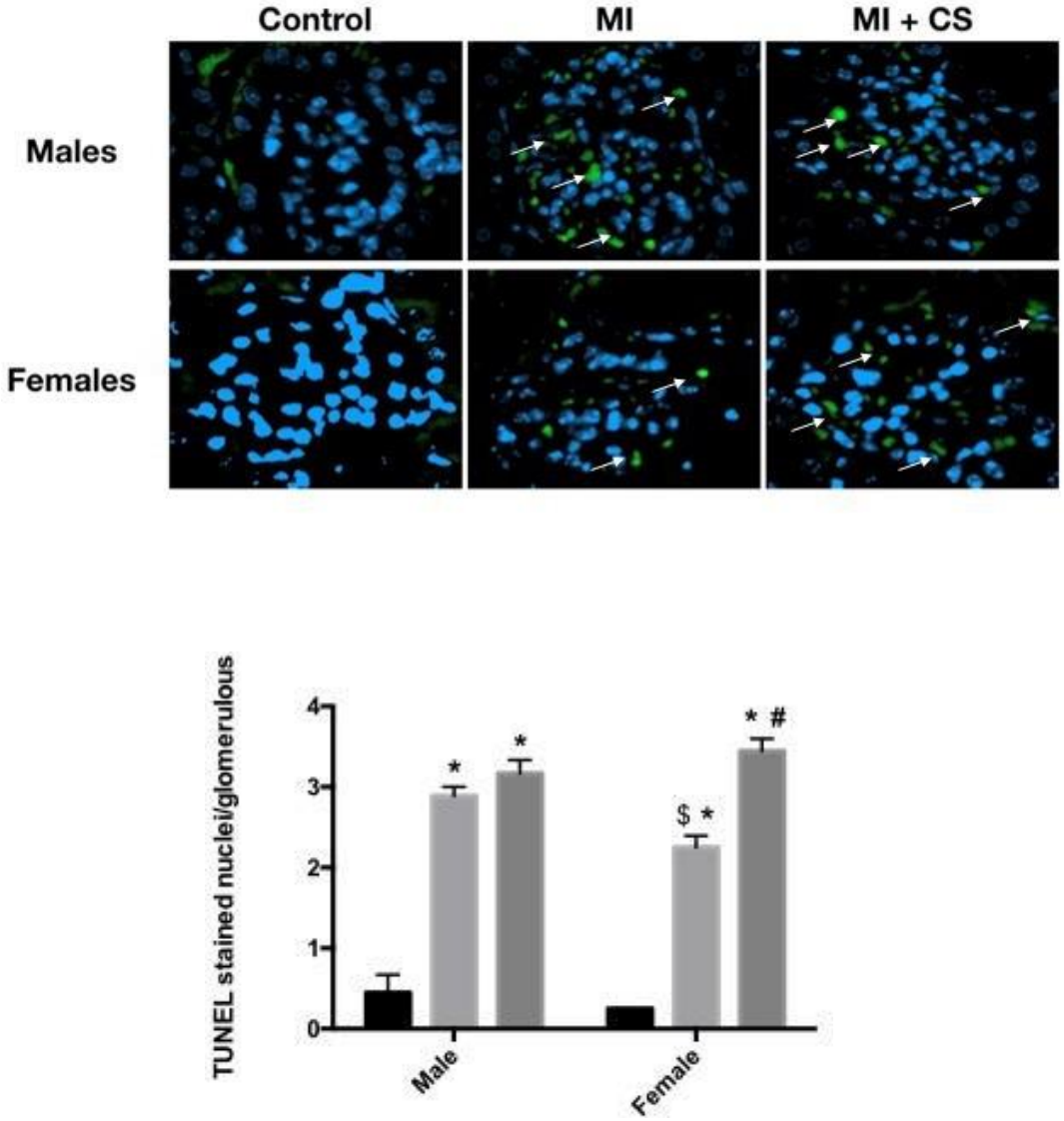

Figure 13 Effect of MI and MI+CS on glomeruli DNA fragmentation

using TUNEL assay: DNA fragmentation was significantly increased in non CS- exposed and CS exposed MI male mice compared to baseline. A significant increase in DNA fragmentation was observed in non CS- exposed and CS- exposed MI female mice compared to baseline and non CS-exposed MI mice respectively. Ctrl: Control; MI: Myocardial infarction; CS: Cigarette smoking; *: Significance between MI and Ctrl; #: Significance between MI+CS and MI; $: Significance between male and female mice; (n=3); Values are represented as mean ± s.e.m.; Two-Way-Anova statistical analysis; P value<0.05.

3. *Evaluation of pro-inflammatory, pro-apoptotic, and anti-inflammatory cytokines protein expression in male and female mice' kidneys tissue*

a. IL-1β was significantly increased in male groups compared to control

Figure 15 shows a significant increase in IL-1β protein level in non-CS exposed and CS-exposed MI male mice compared to their controls. While, no significant change in IL- 1β protein level in female mice was observed.

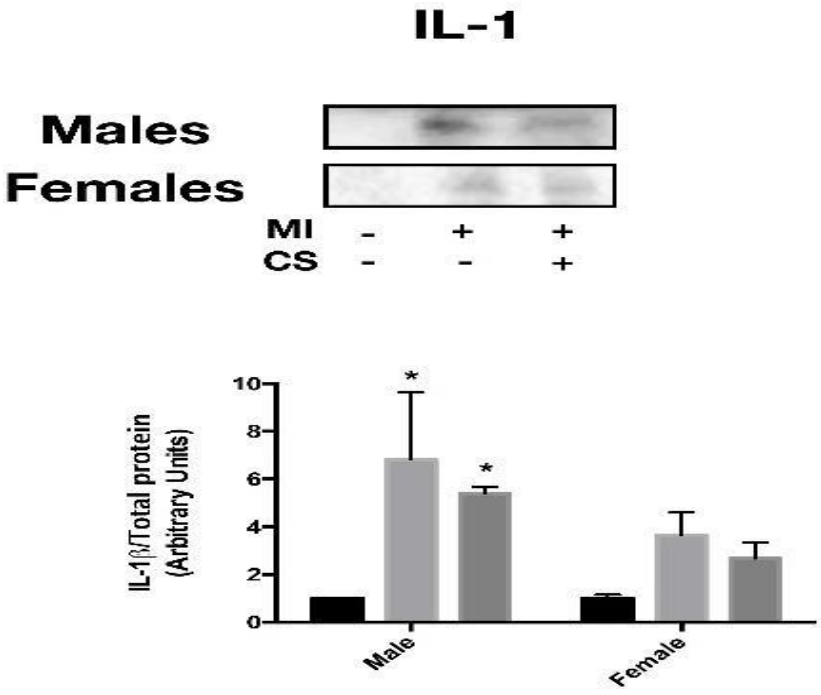

Figure 14 Effect of MI and MI+CS on IL-1 β protein levels

In kidney tissues: Wb showed a significant increase in IL-1β in non and CS- exposed MI male compared to baseline. . Ctrl: control; MI: Myocardial infarction; CS: Cigarette smoking male; *: Significance between MI and Ctrl; (Male groups n=6, Female groups n=4); Values are represented as mean ± s.e.m.; Two-Way-Anova statistical analysis; P value<0.05

b. <u>Significant increase in pro-caspase 3 protein level was noted in non CS-exposed MI male compared to non CS-exposed MI female mice</u>

Figure 16 shows a marked increase in pro-caspase 3 protein level in non CS- exposed MI males compared to the relative female group. CS exposed MI male mice tend to have a higher level of pro-caspase 3 expression when compared to relative female groups.

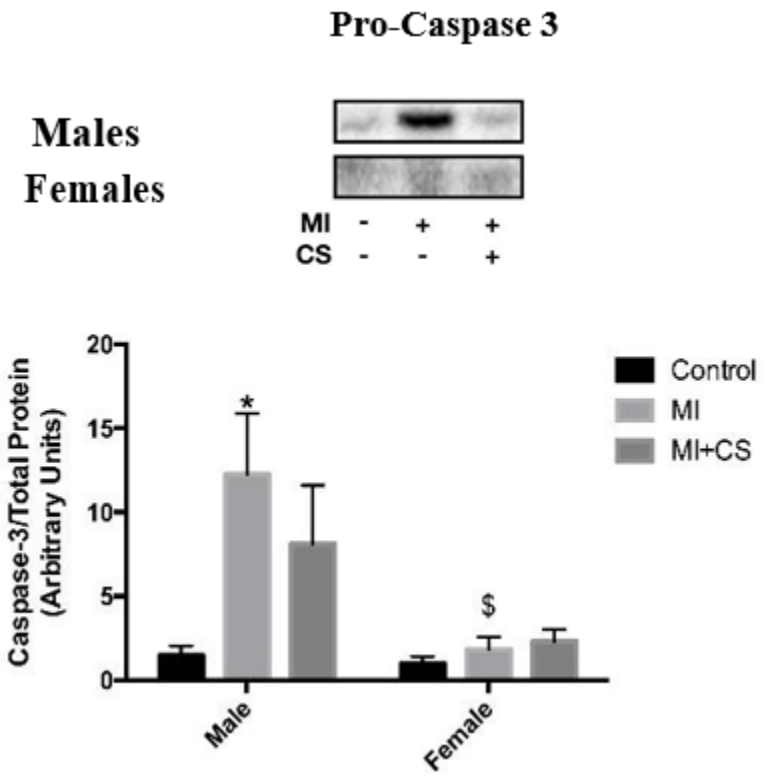

Figure 15 Effect of MI and MI+CS on pro-caspase 3 protein level

In kidney tissues: Wb showed a significant increase in pro- caspase 3 level in non CS-exposed MI male compared to non CS-exposed MI female mice. Ctrl: control; MI: Myocardial infarction; CS: Cigarette smoking male; *: Significance between MI and Ctrl; $: Significance between male and female mice; (Male groups n=6, Female groups n=4); Values are represented as mean ± s.e.m.; Two-Way- Anova statistical analysis; P value<0.05

c. <u>IL-13 significantly increased in CS-exposed MI female mice when compared to relative MI male mice groups.</u>

Figure 17 demonstrates that IL-13 protein level was significantly increased in non CS-exposed and CS-exposed MI female groups compared to control. Of interest, higher level of IL-13 was observed in CS-exposed MI female mice when compared to the relative male subjects.

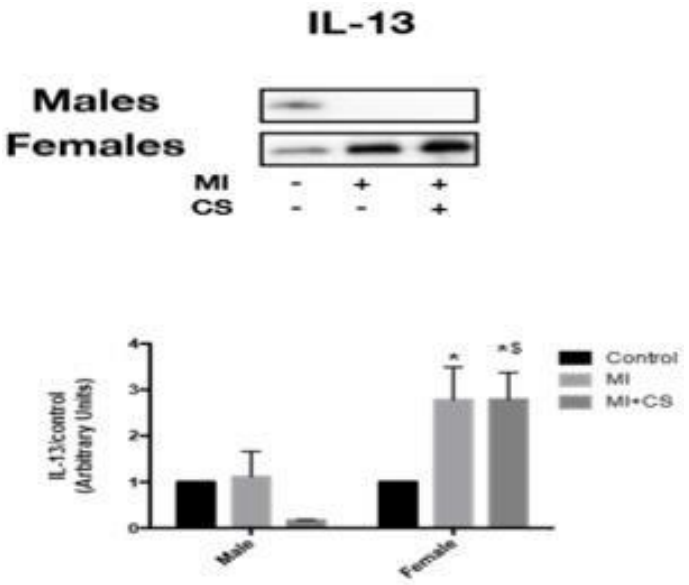

Figure 16 Effect of MI and MI+CS on anti-inflammatory cytokines IL-13 protein

In kidney tissues: Wb showed a significant increase in IL-13 expression level in non CS- exposed and CS- exposed MI females compared to control. Additionally, IL-13 was significantly increased in CS-exposed MI females compared to CS- exposed MI male mice. Ctrl: control; MI: Myocardial infarction; CS: Cigarette smoking male; *: Significance between MI and Ctrl; $: Significance between male and female mice (Male groups n=6, female groups n=4); Values are represented as mean ± s.e.m.; Two-Way-Anova statistical analysis; p value<0.05

d. Significant increase in IL-4 levels in CS-exposed MI female mice compared to control

Figure 18 shows that IL-4 protein level was significantly heightened in non CS-exposed MI male and female mice compared to control. Of note, a marked increase in IL-4 level was also observed in CS-exposed MI female mice when compared to control.

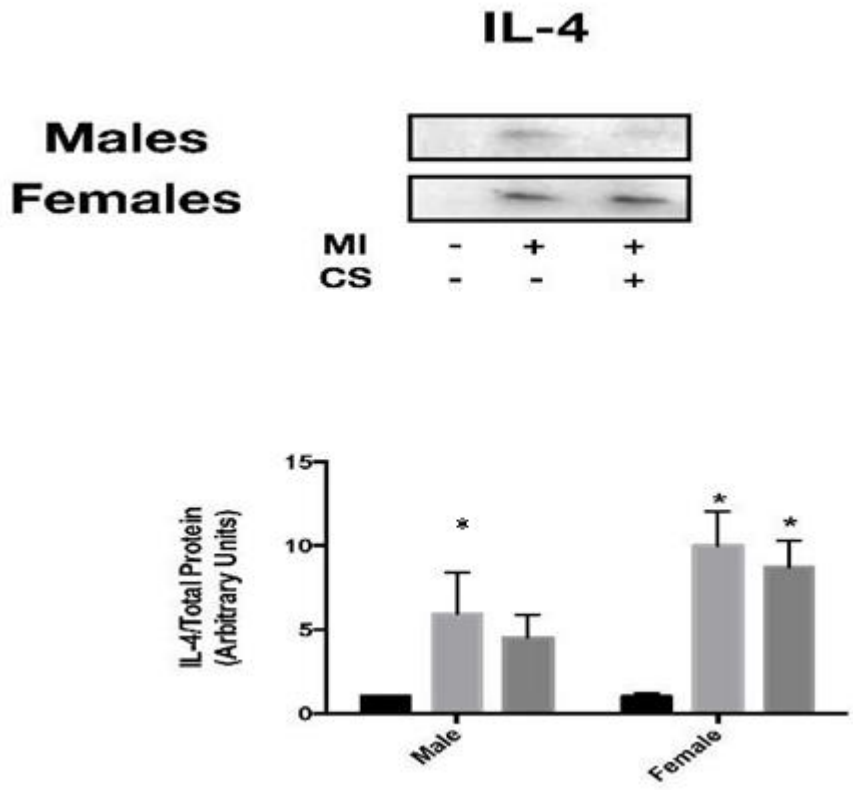

Figure 17 Effect of MI and MI+CS on anti-inflammatory cytokines IL-4 protein level

kidney tissues: Wb showed a significant increase in IL-4 expression level in non CS- exposed male and female mice. Additionally IL-4 was significantly heightened in CS- exposed MI females when compared to control. Ctrl: control; MI: Myocardial infarction; CS: Cigarette smoking male; *: Significance between MI and Ctrl; $: Significance between male and female mice (Male groups n=6, female groups n=4); Values are represented as mean ± s.e.m.; Two-Way-Anova statistical analysis; p value<0.05

e. <u>No significant increase in IL-10 in both gender was noted</u>

Figure 19 shows no significant change in IL-10 protein level in both non and CS-exposed MI genders when compared to their control groups. However, a similar trend to IL-4 expression was observed.

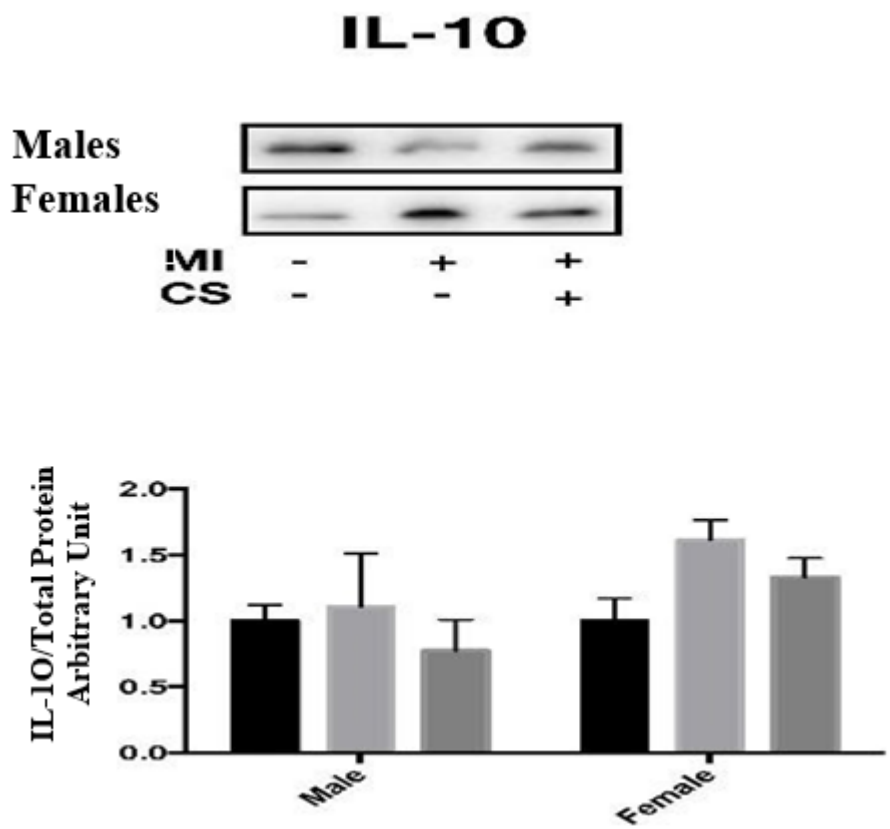

Figure 18 Effect of MI and MI+CS on anti-inflammatory cytokines IL-10 protein level

Kidney tissues: Wb showed that no significant change in IL-10 protein level in non CS- exposed and CS- exposed MI male and female mice was observed. Ctrl: control; MI: Myocardial infarction; CS: Cigarette smoking male; *: Significance between MI and Ctrl; $: Significance between male and female mice (Male groups n=6, female groups n=4); Values are represented as mean ± s.e.m.; Two-Way-Anova statistical analysis; p value<0.05

4. Evaluation of fibrotic biomarkers mRNA expression levels in male and female mice' kidneys tissue

a. <u>MMP 8 and MMP13 expression levels were significantly increased in males when compared to their relative female groups</u>

Figure 20 shows a significant increase in MMP8 mRNA expression level in both non CS-exposed and CS-exposed MI male mice when compared to their relative female groups. MMP13 mRNA expression level, on the other hand, is markedly increased in non CS-exposed MI males when compared to non CS-exposed female mice.

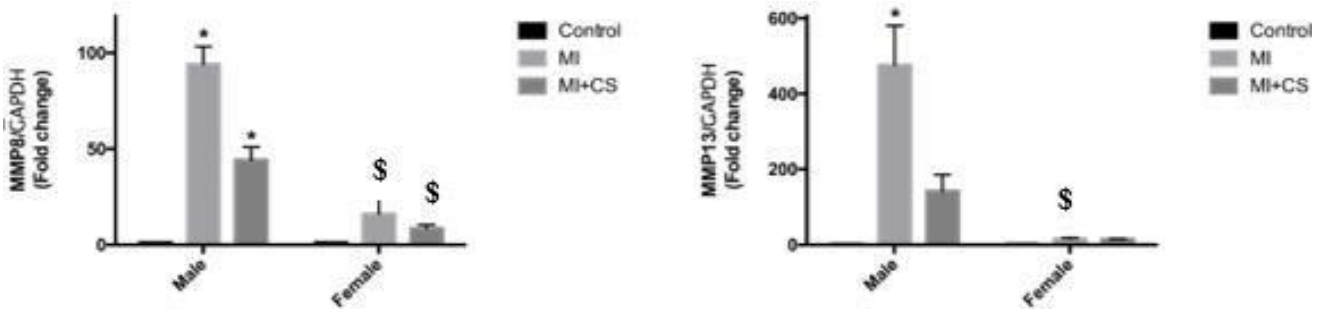

Figure 19 Effect of MI and MI+CS on MMP8 and MMP13 mRNA levels

In kidney tissues: q-PCR showed a significant increase in MMP8 in non CS-exposed and CS- exposed MI male compared to baseline. Additionally, MMP 8 level was markedly heightened in non CS-exposed and CS-exposed MI male when compared to relative female groups. A significant increase in MMP13 m RNA expression level in non CS-exposed MI males compared to non-CS exposed MI female mice was noted. Ctrl: control; MI: Myocardial infarction; CS: Cigarette smoking male;*: Significance between MI and Ctrl; $: Significance between male and female mice (N=3); Values are represented as mean ± s.e.m.; Two-Way-Anova statistical analysis; p value<0.05

b. Connective Tissue Growth Factor (CTGF) and α-Smooth Muscle Actin (α-SMA) mRNA were markedly increased in non-CS exposed MI males when compared to non CS-exposed MI female mice

Figure 21 shows that both CTGF and α-SMA mRNA expression levels markedly heightened in non CS- exposed MI male mice when compared to the relative female groups.

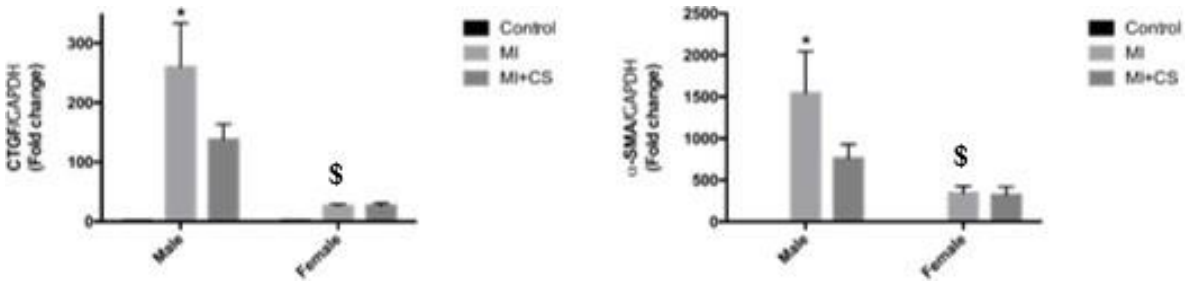

Figure 20 Effect of MI and MI+CS on CTGF and α-SMA mRNA levels

In kidney tissues: q-PCR showed a significant increase in CTGF in non CS-exposed MI male compared the relative female group. α-SMA level was markedly heightened in non CS-exposed MI male when compared to non CS – exposed MI female mice. Ctrl: control; MI: Myocardial infarction; CS: Cigarette smoking male; *: Significance between MI and Ctrl; $: Significance between male and female mice (N=3); Values are represented as mean ± s.e.m.; Two-Way-Anova statistical analysis; p value<0.05.

c. α-Smooth Muscle Actin (α-SMA) protein expression level, using WB and IF, was significantly increased following MI and MI+CS in males when compared to the relative female subjects.

Figure 22 shows that α-SMA protein level markedly heightened in non and CS-exposed MI males when compared to the relative female groups. Of note, no significant change was observed in all female mice groups.

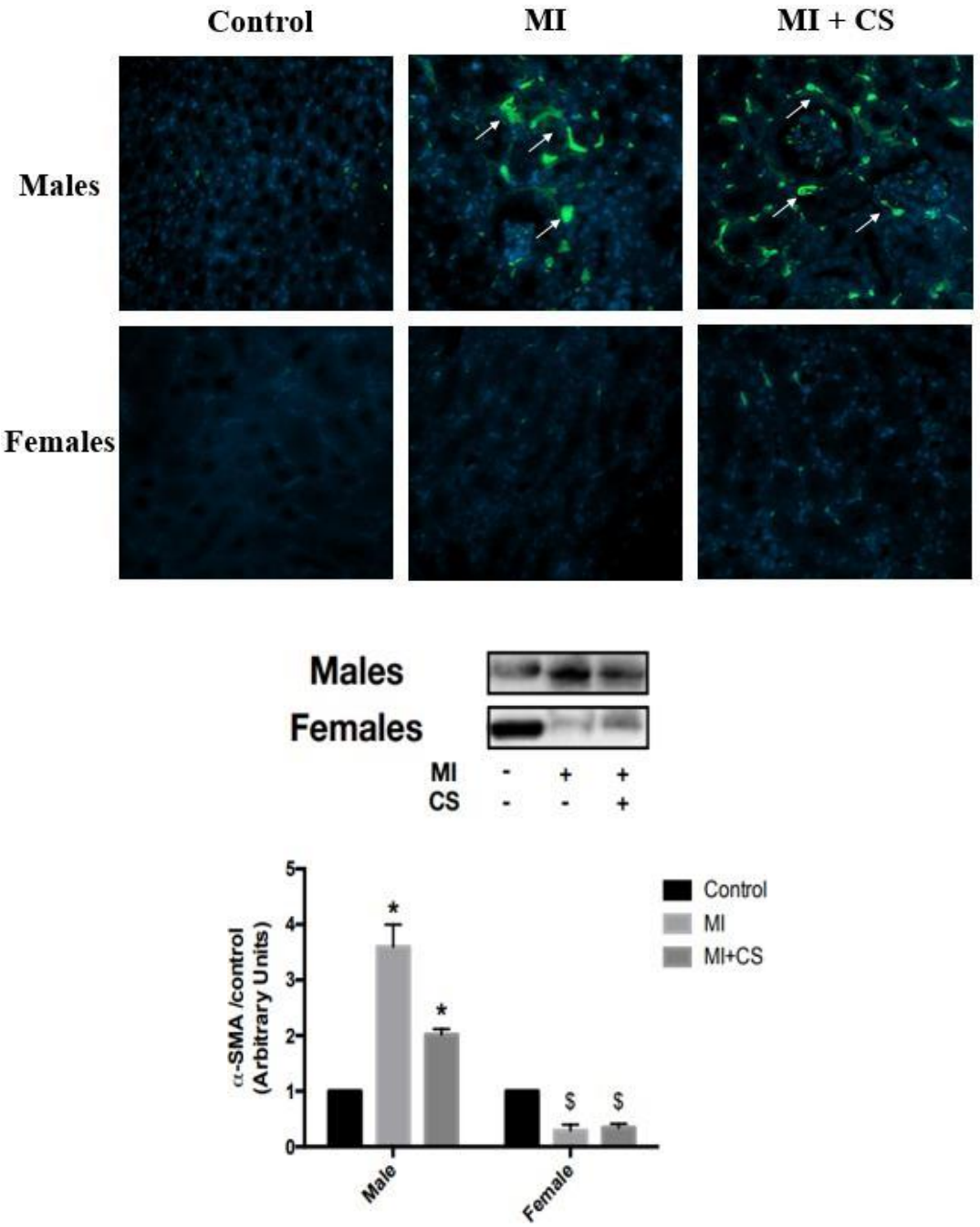

Figure 21 Effect of MI and MI+CS on α-SMA protein level in kidney tissues

WB showed a significant increase in α-SMA in non CS- exposed and CS-exposed MI males when compared control. Of note, α-SMA level was markedly heightened in non and CS- exposed MI males when compared to the relative female subjects. Ctrl: control; MI: Myocardial infarction; CS: Cigarette smoking male; *: Significance between MI and Ctrl; $: Significance between male and female mice (N=3); Values are represented as mean ± s.e.m.; Two-Way-Anova statistical analysis; p value<0.05.

5. ***Evaluation of NAD biosynthetic and consuming enzymes mRNA expression in male and female mice' kidneys tissue***

   a. <u>A significant increase in Nicotine Amide Phosphoribosyl Transferase (NAMPT) and Nicotinamide Riboside Kinase -1 (NMRK-1) in non and CS-exposed MI female mice when compared to the relative male groups</u>

Both NMRK1 and NAMPT mRNA expression levels significantly increased in non and CS-exposed MI females when compared to the relative male mice groups (Figure 23). Male groups, on the other hand show no significant change in NMRK1 and NAMPT mRNA expression levels following MI and MI+CS.

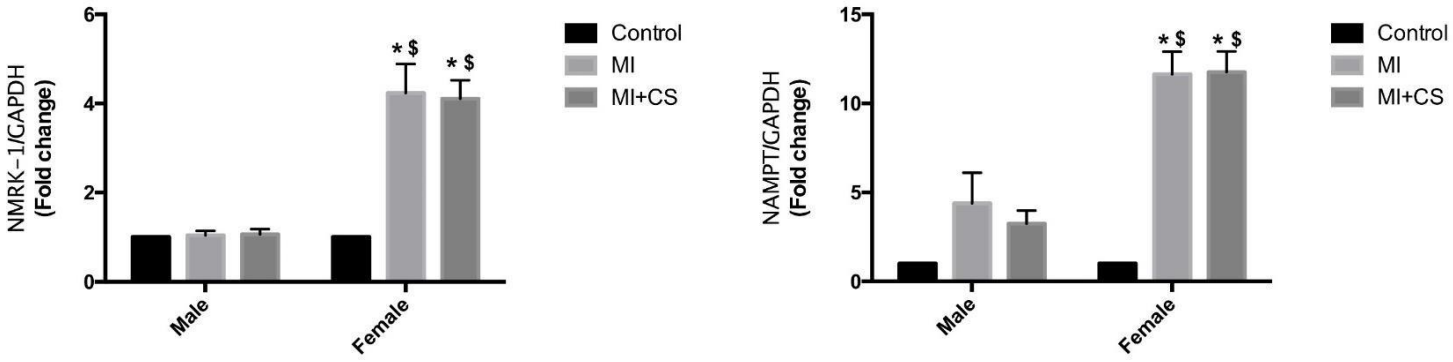

Figure 22 Effect of MI and MI+CS on NMRK-1 and NAMPT mRNA levels

In kidney tissues: q-PCR showed a significant increase in NMRK-1 and NAMPT in non and CS-exposed MI females when compared to the relative male groups. Ctrl: control; MI: Myocardial infarction; CS: Cigarette smoking male; *: Significance between MI and Ctrl; $: Significance between male and female mice (N=3); Values are represented as mean ± s.e.m.; Two-Way-Anova statistical analysis; p value<0.05.

b. <u>SIRT-1 and SIRT-3 were significantly decreased in male mice when compared to the relative female subjects</u>

SIRT1 and SIRT3 mRNA expression levels significantly decreased in CS- exposed MI male mice when compared to the relative female group (Figure 24).

Importantly, much marked decrease in SIRT1 and SIRT3 in non and CS-exposed MI male mice were noticed when compared to the relative female subjects.

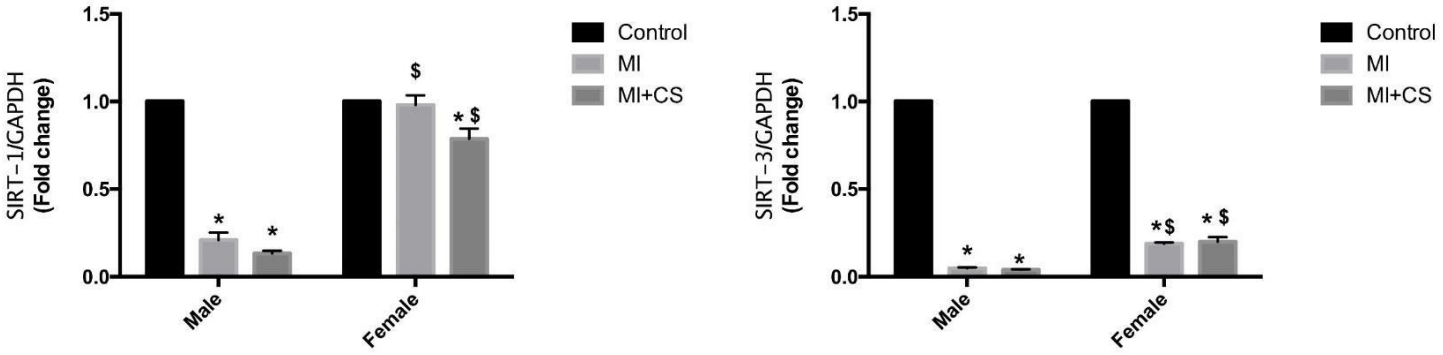

Figure 23 Effect of MI and MI+CS on SIRT-1 and SIRT-3 m RNA level in kidney tissues

q-PCR showed a significant decrease in SIRT1 and SIRT3 expression levels in both genders. Of note, SIRT1 and SIR-3 were markedly decreased in non and CS-exposed MI males when compared to the relative female group. Ctrl: control; MI: Myocardial infarction; CS: Cigarette smoking male; *: Significance between MI and Ctrl; $: Significance between male and female mice (N=3); Values are represented as mean ± s.e.m.; Two-Way-Anova statistical analysis; p value<0.05.

c. <u>Poly (ADP-ribose) polymerase (PARP-1) was significantly heightened in non CS- exposed MI male mice when compared to their relative female group</u>

PARP-1 mRNA expression level significantly increased in non CS-exposed MI males when compare to non CS-exposed MI female mice only.

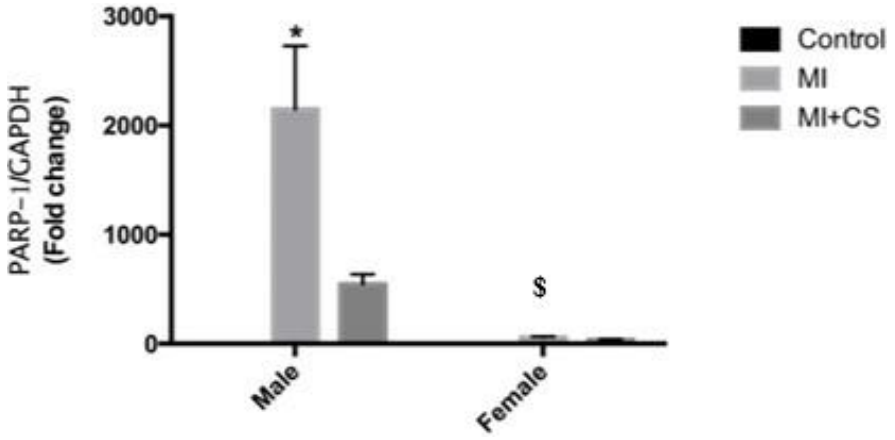

Figure 24 Effect of MI and MI+CS on PARP-1 m RNA level in kidney tissues

q-PCR showed a significant increase in PARP-1 in non CS- exposed MI male compared the relative female group. Ctrl: control; MI: Myocardial infarction; CS: Cigarette smoking male; *: Significance between MI and Ctrl; $: Significance between male and female mice (N=3); Values are represented as mean ± s.e.m.; Two-Way-Anova statistical analysis; p value<0.05.

D. NAD quantification

A Significant decrease in NAD level observed in CS-exposed MI males when compared to non CS-exposed MI male mice.

Figure 26 shows that NAD level significantly decreased in MI male when compared to the control group. Importantly, NAD level is markedly decreased in MI male following CS exposure when compared to MI male mice.

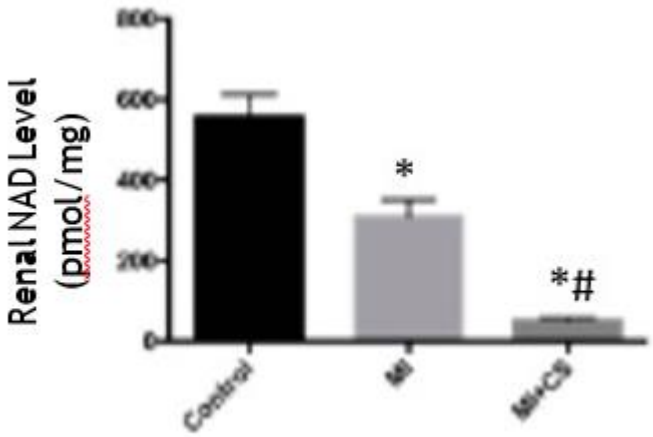

Figure 25 Effect of MI and MI+CS on NAD level

A significant decrease in NAD level in non and CS-exposed MI male compared to the control group. Ctrl: control; MI: Myocardial infarction; CS: Cigarette smoking male; *: Significance between MI and Ctrl; #:Significance between CS-exposed MI male and non CS-exposed MI male mice (N=3); Values are represented as mean ± s.e.m.; One-Way-Anova statistical analysis; p value<0.05.

Chapter IV

DISCUSSION

Type I cardio-renal syndrome is a multifactorial condition in which combined acute cardiac dysfunction and AKI reciprocally amplify the damage of both organs [159]. The pathological mechanisms behind type I CRS development are very complex, including hemodynamic changes, excessive ROS generation, inflammatory response, cell death, and morphological alterations [160]. Numerous studies demonstrated the crucial role of cardio-renal interrelationship in worsened renal damage, where cardiac systolic dysfunction induces enhanced kidney damage. Decreased EF and CO following MI lead to reduced renal perfusion and a subsequent compensatory SNS and RAAS activation [155, 161].

Willemijn et al. showed that activation of RAAS in cardio-renal syndrome was associated with progressive cardiac function loss and heightened renal damage [161]. CS is well- known to have an adverse impact on cardiovascular disease with negative effects on kidneys function [162, 163]. To date, no study compared the impact of CS on MI-induced kidney damage between male and female mice. The main objective of the present study was to assess the potentially different effects of direct CS exposure on kidney function in type I CRS between male and female mice. We report for the first time that CS exacerbates kidney damage following MI in a gender biased manner with females being less susceptible to damage than males. These observations are in accordance with our hemodynamic findings that revealed a worsened ejection fraction in CS exposed MI male when compared to their relative female groups. Findings of this study are not surprising given the repoted impact of CS and/or MI on

kidney damage. Kobeissy et al. reported a marked increase in PCT swelling in CS exposed MI male mice [155]. These claims are in line with our histological results related to kidney damage that revealed a significant increase in glomerular retraction, PCT dilatation, and renal interstitial fibrosis post-MI in both CS-exposed male and female mice. In addition, CS and MI are a major source of ROS induction particularly in the renal cortex supporting glomeruli ROS production that significantly increased in our CS exposed MI groups [164, 165]. Of note, excessive ROS generation caused by endogenous or exogenous stimuli is tightly linked to cellular damage and subsequent induction of inflammatory reaction [108, 166]. Other studies reported findings consistent with our DNA fragmentation data highlighting the stimulatory impact of MI or CS on renal cell death [167] [6]. Independent of the well-known MI and/or CS impact on kidney damage, the main finding of this study is the significant protective effects observed within the kidneys of CS-exposed MI female mice when compared to relative male mice group. These findings are in line with experimental and clinical studies showing a protective effect of female sex hormones on the cardiovascular and renal system. For instance, Wayne et al. reported that enhanced CO, heart rate, oxygen delivery, and decreased systemic vascular resistance are associated with administration of E2 in an animal model with reduced CO [168]. Along the same line, E2 has been shown to reverse endothelial dysfunction via activating endothelial nitric oxide synthase [169]. Endogenous estrogen has also been linked to reduction in glomerular mesangial cells damage, albuminuria, and tubule interstitial fibrosis [151, 170]. Sophie et al. reported that ERαKO female mice developed podocyte apoptosis, resulting in accelerating ECM accumulation and glomerular hypertrophy, eventually increasing albumin excretion and exacerbating kidney damage. Conversely, administration of

E2 inhibits TNF-α induced podocyte apoptosis [171].

At the inflammatory level, our findings indicated a marked increase in IL-1β protein expression level in CS-exposed MI male mice when compared to the relative control, unlike CS-exposed MI female mice that showed no significant difference. Of note, IL-1β levels are implicated in cardiac and renal pathology and accentuated with MI and CS [172, 173] [174] [106, 175]. Targeting IL-1β with a monoclonal antibody decreased cardiovascular events post-MI and enhanced kidney function [176]. Interestingly, previous investigations revealed that physiological concentration of E2 decreases IL-1β expression level and IL-1β/IL-Ar ratio consistent with our observations emphasizing the potential involvement of estrogen in the observed protective effects [177]. IL-13 on the other hand was significantly accentuated in CS-exposed MI female group whereas IL-4 and IL-10 tended to be higher when compared to relative male group indicating anti-inflammatory profile dominance in CS-exposed MI female group. Both IL- 4 and IL-13 are known to promote AKI recovery by enhancing macrophage polarization to M2 phenotype [178, 179]. In their study, Zang et al. reported that IL-4/IL-13 inhibition enhances tubular injury along with decreased M2 anti-inflammatory phenotype and enhanced M1 pro-inflammatory phenotype and subsequent increase in renal interstitial fibrosis. IL-4 and IL-13 up-regulation in female mice can also be linked to estrogen [178]. In fact, Campbell et al. indicated that IL-4-induced M2 polarization is primed in the presence of E2 in mouse bone marrow derived macrophages (BMMs) [180]. Additionally, Riffo et al. demonstrated that clinically relevant concentration of E2 promotes IL-13 expression level in mediastinal lymph node cultures [181]. Noteworthy, no significant change in renal IL-10 expression level was observed between male and female mice following MI and MI+CS when

compared to relative controls. These results correlate with a study done by Zymek et al. indicating that IL-10 has no central role in suppressing pro- inflammation cytokines release and fibrosis deposition following MI [182].

With respect to our pro-fibrotic biomarkers findings, both Carig et al. and Garcia et al. reported that MPP8 -/- mice showed reduced fibrosis, indicating that MMP8 has a pro- fibrotic effect which was linked in our result to worsened kidney damage in CS-exposed MI male when compared to the relative female group [183] [184]. As for MMP13 and CTGF levels, George et al., showed that MMP13 cleaves CTGF, releasing therefore bioactive fragments that are implicated in the progression of fibrosis [185]. Similarly, α- SMA, the hallmark of fibroblast –to-myofibroblast differentiation and fibrosis, significantly increased in CS-exposed MI male mice when compared to CS-exposed MI female group. The observed pro-fibrotic biomarkers levels elaborate on the observed worsened kidney damage in CS-exposed MI male group [186]. Additionally, the anti- inflammatory cytokine IL-13, markedly increased in CS-exposed MI female mice, is known to downregulate MMP13 mRNA and protein levels, eventually decreasing CTGF and α-SMA levels [187]. In contrast, the pro-inflammatory cytokine IL-1β was shown to induce MMP8 and MMP13 mRNA expression level in gingival fibroblast, leading to increase fibrosis [188]. These claims are in accordance with our findings showing that increased IL-1β protein expression level in male mice following MI/CS tightly correlated with heightened renal interstitial fibrosis [182].

Metabolically, our findings revealed that both NMRK1 and NAMPT, NAD biosynthetic enzymes, were markedly heightened in females following MI and MI+CS when compared to the relative male groups. Veer et al and Pillai et al reported that increased

NAMPT expression level enhances cellular life span through inducing SIRT1 mediated-mitochondrial protein deacetylation and inhibiting PARP1-induced energy failure and cell death [189, 190]. Similarly, Ratajczak et al. indicated that NMRK1 is highly expressed in kidney tissues [191]. NMRK1 activity is required for the conversion of the exogenous supplementation nicotinamide riboside (NR) to nicotinamide mononucleotide (NMN), and subsequently to NAD [192]. Together SIRT1 and SIRT3, both being NAD dependent enzymes, are implicated in mitochondria proteins deacetylation and integrity and were significantly decreased in both MI male and female mice following CS exposure. Noteworthy, this decrease was markedly heightened in CS- exposed MI males when compared to their relative female group. Our data are consistent with multiple studies correlating renal stress with decreased SIRT1 and SIRT3 mRNA expression levels. A model of diabetic nephropathy induced AKI showed a significant decrease in SIRT3 mRNA expression level, resulting in mesangial cells hypertrophy [193]. Similarly, decreased SIRT3 mRNA expression level along with mitochondrial protein hyperacetylation are documented in a model of cystatin- induced AKI [194]. Multiple early studies linked SIRT-1 to mitochondria biogenesis, enhanced podocytes function, decreased renal inflammation, fibrosis, and apoptosis [195, 196]. E2 is known to promote the expression of SIRT-1 in response to excessive ROS generation, resulting in caspase-3 inhibition, subsequently decrease in cell death [197]. Additionally, Capllonch et al. indicated that the expression of SIRT3 is primed in ovariectomized female mice treated with E2 [198]. On the other hand, PARP-1, a NAD consuming enzyme known to be involved in several kidney disease models, tended to be higher in CS-exposed MI male mice when compared to their relative female group without reaching significance. Our NAD

data revealed a significant decrease in NAD levels following CS exposure in MI male mice supporting the potential hypothesis behind PARP-1 mediated NAD depletion and the mitochondria-associated cell death. The causative or associative relationship between inflammation and NAD deficiency-induced apoptosis/necrosis cannot be ascertained based on our findings. Further experiments using the PARP-1 inhibitor rucaparib, or direct targeting of IL-1β, for instance, by canakinumab might be necessary to sort this question.

In summary, this is the first study to report gender-biased differences in kidney damage emphasizing a pronounced renal protection in CS-exposed MI female mice when compared to relative male group with potential links to estrogen protective effects. However, whether the observed findings are mainly due to estrogen mediated protection on the heart or kidney or both is not clear. Our cardiac hemodynamic analysis revealed a worsened cardiac function in CS exposed MI-male mice when compared to relative female group with no difference between both genders when exposed to MI only, indicating a CS- exposed genders difference at least at the cardiac level. Whether the observed differences at the heart level are translated onto the kidney due to worsened CO only in CS-exposed MI male mice, requires further investigation. Of note blood pressure in both genders was similar in the presence and absence of CS and prior to MI induction indicating that any observed difference in cardiac function in MI males and females is CS-mediated potentially through direct impact on the myocardium. Ovarectomy and CS exposed controls studies will reveal whether estrogen is involved in these observed effects and whether CS-induced damage on kidneys in type1 CRS is mediated through cardiac or renal alteration mechanisms or both.

REFERENCES

1. Volpe, M., Natriuretic peptides and cardio-renal disease. International journal of cardiology, 2014. 176(3): p. 630-639.
2. House, A.A., et al., Therapeutic strategies for heart failure in cardiorenal syndromes. American Journal of Kidney Diseases, 2010. 56(4): p. 759-773.
3. Altara, R., et al., Temporal cardiac remodeling post-myocardial infarction: dynamics and prognostic implications in personalized medicine. Heart failure reviews, 2016. 21(1): p. 25
4. Ronco, C., et al., Cardiorenal syndrome. J Am Coll Cardiol, 2008. 52(19): p. 1527-39.
5. Butler, J., et al., Relationship between heart failure treatment and development of worsening renal function among hospitalized patients. Am Heart J, 2004. 147(2): p. 331-8.
6. Pastori, S., et al., Cardiorenal syndrome type 1: activation of dual apoptotic pathways. Cardiorenal medicine, 2015. 5(4): p. 306-315.
7. D'Antono, B., et al., Cardiopulmonary baroreflex stimulation and blood pressure-related hypoalgesia. Biological psychology, 2000. 53(2-3): p. 217-231.
8. Boudoulas, K.D., et al., The cardio-renal interrelationship. Progress in cardiovascular diseases, 2017. 59(6): p. 636-648.
9. Lohse, M.J., S. Engelhardt, and T. Eschenhagen, What is the role of β-adrenergic signaling in heart failure? Circulation research, 2003. 93(10): p. 896-906.
10. Saxena, P.R., Interaction between the renin-angiotensin-aldosterone and sympathetic nervous systems. Journal of cardiovascular pharmacology, 1992. 19: p. S80-8.
11. Fyhrquist, F., K. Metsärinne, and I. Tikkanen, Role of angiotensin II in blood pressure regulation and in the pathophysiology of cardiovascular disorders. Journal of human hypertension, 1995. 9: p. S19-24.
12. Smith, G.L., et al., Renal impairment and outcomes in heart failure: systematic review and meta-analysis. Journal of the American College of Cardiology, 2006. 47(10): p. 1987-1996.
13. Heywood, J.T., et al., High prevalence of renal dysfunction and its impact on outcome in 118,465 patients hospitalized with acute decompensated heart failure: a report from the ADHERE database. Journal of cardiac failure, 2007. 13(6): p. 422-430.
14. Cowie, M.R., et al., Prevalence and impact of worsening renal function in patients hospitalized with decompensated heart failure: results of the prospective outcomes study in heart failure (POSH). Eur Heart J, 2006. 27(10): p. 1216-22.
15. McCullough, P.A., Cardiorenal syndromes: pathophysiology to prevention. Int J Nephrol,2010. 2011: p. 762590.
16. Frangogiannis, N.G., C.W. Smith, and M.L. Entman, The inflammatory response in myocardial infarction. Cardiovasc Res, 2002. 53(1): p. 31-47.
17. Kaplan, A., et al., Functional, cellular, and molecular remodeling of the heart under influence of oxidative cigarette tobacco smoke. Oxidative medicine and cellular longevity, 2017. 2017.
18. Velazquez, E.J., et al., Coronary-artery bypass surgery in patients with ischemic

cardiomyopathy. New England Journal of Medicine, 2016. 374(16): p. 1511-1520.
19. Johnson, R.J., et al., Tubulointerstitial injury and loss of nitric oxide synthases parallel the development of hypertension in the Dahl-SS rat. J Hypertens, 2000. 18(10): p. 1497-505.
20. Deedwania, P.C. and E.V. Carbajal, Silent myocardial ischemia. A clinical perspective. Arch Intern Med, 1991. 151(12): p. 2373-82.
21. Reckelhoff, J.F. and W.K. Samson, Sex and gender differences in cardiovascular, renal and metabolic diseases. Am J Physiol Regul Integr Comp Physiol, 2015. 309(9): p. R1057-9.
22. Lerner, D.J. and W.B. Kannel, Patterns of coronary heart disease morbidity and mortality in the sexes: a 26-year follow-up of the Framingham population. Am Heart J, 1986. 111(2):p. 383-90.
23. Khan, R.J., et al., Relationship between obesity and coronary heart disease among urban Bangladeshi men and women. Integrative obesity and diabetes, 2015. 1(3): p. 49.
24. Schargrodsky, H., et al., Body weight and nonfatal myocardial infarction in a case-control study from Argentina. Sozial-und Präventivmedizin, 1994. 39(3): p. 126-133.
25. Zhu, J., et al., The incidence of acute myocardial infarction in relation to overweight and obesity: a meta-analysis. Archives of medical science: AMS, 2014. 10(5): p. 855.
26. Pearson, T.A., et al., Markers of inflammation and cardiovascular disease: application to clinical and public health practice: a statement for healthcare professionals from the Centers for Disease Control and Prevention and the American Heart Association. Circulation, 2003. 107(3): p. 499-511.
27. Gupta, R., et al., Bodymass index, waist-size, waist-hip ratio and cardiovascular risk factors in urban subjects. Japi, 2007. 55: p. 621-627.
28. Williams, K.J. and I. Tabas, Lipoprotein retention—and clues for atheroma regression. 2005, Am Heart Assoc.
29. Rajala, M.W. and P.E. Scherer, Minireview: the adipocyte—at the crossroads of energy homeostasis, inflammation, and atherosclerosis. Endocrinology, 2003. 144(9): p. 3765-3773.
30. Wang, Z. and T. Nakayama, Inflammation, a link between obesity and cardiovascular disease. Mediators of inflammation, 2010. 2010.
31. Williams, K.J. and I. Tabas, The response-to-retention hypothesis of atherogenesis reinforced. Current opinion in lipidology, 1998. 9(5): p. 471-474.
32. Shoelson, S.E., J. Lee, and A.B. Goldfine, Inflammation and insulin resistance. The Journal of clinical investigation, 2006. 116(7): p. 1793-1801.
33. Gomes, M.d.B., Impact of diabetes on cardiovascular disease: an update. International journal of hypertension, 2013. 2013.
34. Chait, A., et al., Thematic review series: the immune system and atherogenesis. Lipoprotein-associated inflammatory proteins: markers or mediators of cardiovascular disease? Journal of Lipid Research, 2005. 46(3): p. 389-403.
35. Leon, B.M. and T.M. Maddox, Diabetes and cardiovascular disease: Epidemiology, biological mechanisms, treatment recommendations and future research. World journal of diabetes, 2015. 6(13): p. 1246.
36. Kannel, W.B. and D.L. McGee, Diabetes and cardiovascular disease: the Framingham study. Jama, 1979. 241(19): p. 2035-2038.
37. Legato, M.J., Cardiovascular disease in women: what's different? What's new? What's

unresolved? Annals of the New York Academy of Sciences, 1994. 736(1): p. 147-157.
38. Yusuf, S., et al., Effect of potentially modifiable risk factors associated with myocardial infarction in 52 countries (the INTERHEART study): case-control study. The lancet, 2004.364(9438): p. 937-952.
39. Jones, C.A. and S. Nagpal, An update: women, hypertension and therapeutic efficacy. The Canadian journal of cardiology, 2001. 17(12): p. 1283-1289.
40. Os, I., et al., Sex differences in essential hypertension. Journal of internal medicine, 1993.233(1): p. 13-19.
41. Maric, C., Sex differences in cardiovascular disease and hypertension: involvement of the renin-angiotensin system. Hypertension, 2005. 46(3): p. 475-476.
42. McDonald, M., et al., Prevalence, awareness, and management of hypertension, dyslipidemia, and diabetes among United States adults aged 65 and older. Journals of Gerontology Series A: Biomedical Sciences and Medical Sciences, 2009. 64(2): p. 256-263.
43. Hertz, R.P., et al., Racial disparities in hypertension prevalence, awareness, and management. Archives of internal medicine, 2005. 165(18): p. 2098-2104.
44. Lacruz, M.E., et al., Prevalence and incidence of hypertension in the general adult population: results of the CARLA-cohort study. Medicine, 2015. 94(22).
45. Tomek, J. and G. Bub, Hypertension-induced remodelling: on the interactions of cardiac risk factors. The Journal of physiology, 2017.
46. Frohlich, E.D., An updated concept for left ventricular hypertrophy risk in hypertension.The Ochsner Journal, 2009. 9(4): p. 181-190.
47. Mendis, S., et al., Global atlas on cardiovascular disease prevention and control. 2011: Geneva: World Health Organization.
48. Service, U.P.H., The health consequences of smoking. A report to the Surgeon General: 1971. Washington, DC: US Department of Health, Education and Welfare. Public Health Service, Publication (HSM), 1972: p. 71-7513.
49. Burns, D.M., Epidemiology of smoking-induced cardiovascular disease. Progress in cardiovascular diseases, 2003. 46(1): p. 11-29.
50. Tang, J.-l. and J.A. Dickinson, Smoking and risk of myocardial infarction. Bmj, 1998. 317(7164): p. 1018.
51. Fagerstrom, K., The epidemiology of smoking: health consequences and benefits of cessation. Drugs, 2002. 62 Suppl 2: p. 1-9.
52. Samet, J.M. and H.L. Wipfli, Globe still in grip of addiction. Nature, 2010. 463(7284): 1020.
53. Renna, N.F., N. de las Heras, and R.M. Miatello, Pathophysiology of vascular remodeling in hypertension. International journal of hypertension, 2013. 2013.
54. Control, C.f.D. and Prevention, The health consequences of smoking—50 years of progress: a report of the Surgeon General. Atlanta (GA): US Department of Health and Human Services, 2014.
55. Huang, M.F., W.L. Lin, and Y.C. Ma, A study of reactive oxygen species in mainstream of
cigarette. Indoor Air, 2005. 15(2): p. 135-40.
56. Jain, G. and E.A. Jaimes, Nicotine signaling and progression of chronic kidney disease in smokers. Biochemical pharmacology, 2013. 86(8): p. 1215-1223.

57. Jain, G. and E.A. Jaimes, Nicotine signaling and progression of chronic kidney disease in smokers. Biochem Pharmacol, 2013. 86(8): p. 1215-23.
58. Hori, M. and K. Nishida, Oxidative stress and left ventricular remodelling after myocardial infarction. Cardiovascular research, 2008. 81(3): p. 457-464.
59. Velagaleti, R.S., et al., Long-term trends in the incidence of heart failure after myocardial infarction. Circulation, 2008. 118(20): p. 2057-62.
60. Altara, R., et al., Temporal cardiac remodeling post-myocardial infarction: dynamics and prognostic implications in personalized medicine. Heart Fail Rev, 2015.
61. Whelan, R.S., V. Kaplinskiy, and R.N. Kitsis, Cell death in the pathogenesis of heart disease: mechanisms and significance. Annu Rev Physiol, 2010. 72: p. 19-44.
62. Rossen, R.D., et al., Mechanism of complement activation after coronary artery occlusion: evidence that myocardial ischemia in dogs causes release of constituents of myocardial subcellular origin that complex with human C1q in vivo. Circ Res, 1988. 62(3): p. 572-84.
63. Frantz, S., J. Bauersachs, and G. Ertl, Post-infarct remodelling: contribution of wound healing and inflammation. Cardiovasc Res, 2009. 81(3): p. 474-81.
64. Nian, M., et al., Inflammatory cytokines and postmyocardial infarction remodeling. Circ Res, 2004. 94(12): p. 1543-53.
65. Brown, R.D., et al., The cardiac fibroblast: therapeutic target in myocardial remodeling and failure. Annu Rev Pharmacol Toxicol, 2005. 45: p. 657-87.
66. Fedak, P.W., et al., Cardiac remodeling and failure: from molecules to man (Part I). Cardiovasc Pathol, 2005. 14(1): p. 1-11.
67. Siwik, D.A., D.L. Chang, and W.S. Colucci, Interleukin-1beta and tumor necrosis factor- alpha decrease collagen synthesis and increase matrix metalloproteinase activity in cardiac fibroblasts in vitro. Circ Res, 2000. 86(12): p. 1259-65.
68. Whittaker, P., D.R. Boughner, and R.A. Kloner, Role of collagen in acute myocardial infarct expansion. Circulation, 1991. 84(5): p. 2123-34.
69. Goldhaber, J.I., Free radicals enhance Na+/Ca2+ exchange in ventricular myocytes. Am JPhysiol, 1996. 271(3 Pt 2): p. H823-33.
70. Yokoyama, T., et al., Cellular basis for the negative inotropic effects of tumor necrosis factor-alpha in the adult mammalian heart. J Clin Invest, 1993. 92(5): p. 2303-12.
71. Di Lullo, L., et al., Pathophysiology of the cardio-renal syndromes types 1-5: An uptodate.Indian Heart J, 2017. 69(2): p. 255-265.
72. Li, Z., et al., Identification and predicting short-term prognosis of early cardiorenal syndrome type 1: KDIGO is superior to RIFLE or AKIN. PLoS One, 2014. 9(12): p. e114369.
73. Forman, D.E., et al., Incidence, predictors at admission, and impact of worsening renal function among patients hospitalized with heart failure. Journal of the American College of Cardiology, 2004. 43(1): p. 61-67.
74. Adams, K.F., et al., Characteristics and outcomes of patients hospitalized for heart failure in the United States: rationale, design, and preliminary observations from the first 100,000 cases in the Acute Decompensated Heart Failure National Registry (ADHERE). American heart journal, 2005. 149(2): p. 209-216.
75. Fiksen-Olsen, M.J., et al., Renal effects of angiotensin II inhibition during increases in renal venous pressure. Hypertension, 1992. 19(2 Suppl): p. II137.

76. Taddei, S., et al., Vascular renin-angiotensin system and neurotransmission in hypertensive persons. Hypertension, 1991. 18(3): p. 266-277.
77. Triposkiadis, F., et al., Reframing the association and significance of co-morbidities in heart failure. Eur J Heart Fail, 2016. 18(7): p. 744-58.
78. Lewis, T., A Clinical Lecture ON PAROXYSMAL DYSPNOEA IN CARDIORENAL PATIENTS: WITH SPECIAL REFERENCE TO "CARDIAC" AND "URAEMIC" ASTHMA: Delivered at University College Hospital, London, November 12th, 1913. Br Med J, 1913. 2(2761): p.1417-20.
79. Charloux, A., et al., Mechanisms of renal hyporesponsiveness to ANP in heart failure. Eur JClin Invest, 2003. 33(9): p. 769-78.
80. Ismail, Y., et al. Cardio-renal syndrome type 1: epidemiology, pathophysiology, and treatment. in Seminars in nephrology. 2012. Elsevier.
81. Virzi, G.M., et al., Oxidative stress: dual pathway induction in cardiorenal syndrome type 1 pathogenesis. Oxid Med Cell Longev, 2015. 2015: p. 391790.
82. Nian, M., et al., Inflammatory cytokines and postmyocardial infarction remodeling. Circulation research, 2004. 94(12): p. 1543-1553.
83. Metra, M., et al., Worsening renal function in patients hospitalised for acute heart failure: clinical implications and prognostic significance. European journal of heart failure, 2008.10(2): p. 188-195.
84. Testani, J.M., et al., Potential effects of aggressive decongestion during the treatment of decompensated heart failure on renal function and survival. Circulation, 2010. 122(3): p. 265-272.
85. Mishra, J., et al., Neutrophil gelatinase-associated lipocalin (NGAL) as a biomarker for acute renal injury after cardiac surgery. The Lancet, 2005. 365(9466): p. 1231-1238.
86. Mishra, J., et al., Identification of neutrophil gelatinase-associated lipocalin as a novel early urinary biomarker for ischemic renal injury. Journal of the American Society of Nephrology, 2003. 14(10): p. 2534-2543.
87. Han, W.K., et al., Urinary biomarkers in the early detection of acute kidney injury after cardiac surgery. Clinical Journal of the American Society of Nephrology, 2009. 4(5): p. 873-882.
88. Brisco, M.A. and J.M. Testani, Novel renal biomarkers to assess cardiorenal syndrome. Current heart failure reports, 2014. 11(4): p. 485-499.
89. Knight, E.L., et al., Factors influencing serum cystatin C levels other than renal function and the impact on renal function measurement. Kidney international, 2004. 65(4): p. 1416-1421.
90. Dupont, M., et al., Lack of concordance in defining worsening renal function by rise in creatinine vs rise in cystatin C. Congestive Heart Failure, 2013. 19(4).
91. Shemesh, O., et al., Limitations of creatinine as a filtration marker in glomerulopathic patients. Kidney international, 1985. 28(5): p. 830-838.
92. Stevens, L.A., et al., Assessing kidney function—measured and estimated glomerular filtration rate. New England Journal of Medicine, 2006. 354(23): p. 2473-2483.
93. Branten, A.J., G. Vervoort, and J.F. Wetzels, Serum creatinine is a poor marker of GFR in nephrotic syndrome. Nephrology Dialysis Transplantation, 2005. 20(4): p. 707-711.
94. Chernecky, C.C. and B.J. Berger, Laboratory tests and diagnostic procedures. 2007:

Elsevier Health Sciences.
95. Gu, L., et al., Cigarette smoke-induced left ventricular remodelling is associated with activation of mitogen-activated protein kinases. European journal of heart failure, 2008. 10(11): p. 1057-1064.
96. Talukder, M.H., et al., Chronic cigarette smoking causes hypertension, increased oxidative stress, impaired NO bioavailability, endothelial dysfunction, and cardiac remodeling in mice. American Journal of Physiology-Heart and Circulatory Physiology, 2010. 300(1): p. H388-H396.
97. Gvozdjakova, A., et al., Smoke cardiomyopathy: disturbance of oxidative processes in myocardial mitochondria. Cardiovascular research, 1984. 18(4): p. 229-232.
98. Devasagayam, T., et al., Free radicals and antioxidants in human health: current status and future prospects. Japi, 2004. 52(794804): p. 4.
99. Duarte, D.R., et al., The role of oxidative stress and lipid peroxidation in ventricular remodeling induced by tobacco smoke exposure after myocardial infarction. Clinics, 2009. 64(7): p. 691-697.
100. Santos, P.P., et al., The role of lipotoxicity in smoke cardiomyopathy. PloS one, 2014. 9(12): p. e113739.
101. Bozkurt, B., et al., Pathophysiologically relevant concentrations of tumor necrosis factor-α promote progressive left ventricular dysfunction and remodeling in rats. Circulation, 1998.97(14): p. 1382-1391.
102. Torre-Amione, G., et al., Proinflammatory cytokine levels in patients with depressed left ventricular ejection fraction: a report from the Studies of Left Ventricular Dysfunction (SOLVD). Journal of the American College of Cardiology, 1996. 27(5): p. 1201-1206.
103. Chung, K.F., Inflammatory mediators in chronic obstructive pulmonary disease. Current Drug Targets-Inflammation & Allergy, 2005. 4(6): p. 619-625.
104. Mossman, B.T., K.M. Lounsbury, and S.P. Reddy, Oxidants and signaling by mitogen-activated protein kinases in lung epithelium. American journal of respiratory cell and molecular biology, 2006. 34(6): p. 666-669.
105. Walters, M.J., et al., Cigarette smoke activates human monocytes by an oxidant-AP-1 signaling pathway: implications for steroid resistance. Molecular pharmacology, 2005. 68(5): p. 1343-1353.
106. Zhou, X., et al., Trimetazidine protects against smoking-induced left ventricular remodeling via attenuating oxidative stress, apoptosis, and inflammation. PloS one, 2012. 7(7): p. e40424.
107. Gascoigne, N.R. and E. Palmer, Signaling in thymic selection. Curr Opin Immunol, 2011.23(2): p. 207-12.
108. Das, A., et al., Molecular and cellular mechanisms of cigarette smoke-induced myocardial injury: prevention by vitamin C. PLoS One, 2012. 7(9): p. e44151.
109. Zhou, X., G. An, and J. Chen, Hydrogen sulfide improves left ventricular function in smoking rats via regulation of apoptosis and autophagy. Apoptosis, 2014. 19(6): p. 998-1005.
110. Mailloux, R.J., S.L. McBride, and M.-E. Harper, Unearthing the secrets of mitochondrial ROS and glutathione in bioenergetics. Trends in biochemical sciences, 2013. 38(12): p.592-602.

111. Ballinger, S.W., et al., Hydrogen peroxide–and peroxynitrite-induced mitochondrial DNA damage and dysfunction in vascular endothelial and smooth muscle cells. Circulation research, 2000. 86(9): p. 960-966.
112. Knight-Lozano, C.A., et al., Cigarette smoke exposure and hypercholesterolemia increase mitochondrial damage in cardiovascular tissues. Circulation, 2002. 105(7): p. 849-854.
113. Gvozdjáková, A., et al., Captopril increased mitochondrial coenzyme Q_ {10} level, improved respiratory chain function and energy production in the left ventricle in rabbits with smoke mitochondrial cardiomyopathy. Biofactors, 1999. 10(1): p. 61-65.
114. Khalil, M.A.M., et al., Cigarette Smoking and Its Hazards in Kidney Transplantation. AdvMed, 2017. 2017: p. 6213814.
115. García-Esquinas, E., et al., Kidney function and tobacco smoke exposure in US adolescents.Pediatrics, 2013. 131(5): p. e1415-e1423.
116. Hallan, S.I. and S.R. Orth, Smoking is a risk factor in the progression to kidney failure. Kidney Int, 2011. 80(5): p. 516-23.
117. Orth, S.R., Smoking and the kidney. J Am Soc Nephrol, 2002. 13(6): p. 1663-72.
118. Liang, K.V., et al., Nodular glomerulosclerosis: renal lesions in chronic smokers mimic chronic thrombotic microangiopathy and hypertensive lesions. Am J Kidney Dis, 2007. 49(4): p. 552-9.
119. Cooper, R.G., Effect of tobacco smoking on renal function. Indian Journal of Medical Research, 2006. 124(3): p. 261.
120. Kurus, M., M. Ugras, and M. Esrefoglu, Effect of resveratrol on tubular damage and interstitial fibrosis in kidneys of rats exposed to cigarette smoke. Toxicol Ind Health, 2009. 25(8): p. 539-44.
121. Liang, K.V., et al., Nodular glomerulosclerosis: renal lesions in chronic smokers mimic chronic thrombotic microangiopathy and hypertensive lesions. American Journal of Kidney Diseases, 2007. 49(4): p. 552-559.
122. Jaimes, E.A., R.X. Tian, and L. Raij, Nicotine: the link between cigarette smoking and the progression of renal injury? Am J Physiol Heart Circ Physiol, 2007. 292(1): p. H76-82.
123. Devasagayam, T.P., et al., Free radicals and antioxidants in human health: current status and future prospects. J Assoc Physicians India, 2004. 52: p. 794-804.
124. Holmstrom, K.M. and T. Finkel, Cellular mechanisms and physiological consequences of redox-dependent signalling. Nat Rev Mol Cell Biol, 2014. 15(6): p. 411-21.
125. Ambrose, J.A. and R.S. Barua, The pathophysiology of cigarette smoking and cardiovascular disease: an update. J Am Coll Cardiol, 2004. 43(10): p. 1731-7.
126. Silverstein, D.M., Inflammation in chronic kidney disease: role in the progression of renal and cardiovascular disease. Pediatr Nephrol, 2009. 24(8): p. 1445-52.
127. Kobeissy, F., et al., Acute Exposure to Cigarette Smoking Followed by Myocardial Infarction Aggravates Renal Damage in an In Vivo Mouse Model. Oxid Med Cell Longev, 2017. 2017: p. 5135241.
128. Sharaf El Din, U.A., M.M. Salem, and D.O. Abdulazim, Stop chronic kidney disease progression: Time is approaching. World J Nephrol, 2016. 5(3): p. 258-73.
129. Hall, M.E., et al., Cigarette smoking and chronic kidney disease in African Americans in the Jackson Heart Study. Journal of the American Heart Association, 2016. 5(6): p.

e003280.
130. Drummond, C.A., et al., Cigarette smoking and cardio-renal events in patients with atherosclerotic renal artery stenosis. PloS one, 2017. 12(3): p. e0173562.
131. Noronha, I.L., C.K. Fujihara, and R. Zatz, The inflammatory component in progressive renal disease—are interventions possible? Nephrology Dialysis Transplantation, 2002. 17(3): p.363-368.
132. Anders, H.J., V. Ninichuk, and D. Schlondorff, Progression of kidney disease: blocking leukocyte recruitment with chemokine receptor CCR1 antagonists. Kidney Int, 2006. 69(1):p. 29-32.
133. Boor, P., T. Ostendorf, and J. Floege, Renal fibrosis: novel insights into mechanisms and therapeutic targets. Nat Rev Nephrol, 2010. 6(11): p. 643-56.
134. Shimamura, T. and A.B. Morrison, A progressive glomerulosclerosis occurring in partial five-sixths nephrectomized rats. The American journal of pathology, 1975. 79(1): p. 95.
135. Arany, I., et al., A novel U-STAT3-dependent mechanism mediates the deleterious effects of chronic nicotine exposure on renal injury. American Journal of Physiology-Renal Physiology, 2011. 302(6): p. F722-F729.
136. Yokoi, H., et al., Role of connective tissue growth factor in fibronectin expression and tubulointerstitial fibrosis. Am J Physiol Renal Physiol, 2002. 282(5): p. F933-42.
137. Jensen, K., et al., General mechanisms of nicotine-induced fibrogenesis. FASEB J, 2012.26(12): p. 4778-87.
138. Eddy, A.A., Molecular basis of renal fibrosis. Pediatr Nephrol, 2000. 15(3-4): p. 290-301.
139. Liu, Y., Cellular and molecular mechanisms of renal fibrosis. Nat Rev Nephrol, 2011. 7(12):p. 684-96.
140. Wang, X., et al., The cellular response to oxidative stress: influences of mitogen-activated protein kinase signalling pathways on cell survival. Biochem J, 1998. 333 (Pt 2): p. 291-300.141. Youle, R.J. and A. Strasser, The BCL-2 protein family: opposing activities that mediate cell death. Nat Rev Mol Cell Biol, 2008. 9(1): p. 47-59.
142. Hong, T., et al., Cordycepin protects podocytes from injury mediated by complements complex C5b-9. Sichuan da xue xue bao. Yi xue ban= Journal of Sichuan University. Medical science edition, 2015. 46(2): p. 173-8, 227.
143. Lan, X., et al., Nicotine induces podocyte apoptosis through increasing oxidative stress.PloS one, 2016. 11(12): p. e0167071.
144. Orth, S.R., Smoking and the kidney. Journal of the American Society of Nephrology, 2002.13(6): p. 1663-1672.
145. Iorga, A., et al., The protective role of estrogen and estrogen receptors in cardiovascular disease and the controversial use of estrogen therapy. Biol Sex Differ, 2017. 8(1): p. 33.
146. Zhang, J.-B. and C.-L. Guo, Protective effect and mechanism of estrogen receptor β on myocardial infarction in mice. Experimental and therapeutic medicine, 2017. 14(2): p. 1315-1320.
147. Mahmoodzadeh, S., et al., Cardiomyocyte-specific estrogen receptor alpha increases angiogenesis, lymphangiogenesis and reduces fibrosis in the female mouse heart post-myocardial infarction. Journal of cell science & therapy, 2014. 5(1): p. 153.

148. Ly, J.D., D.R. Grubb, and A. Lawen, The mitochondrial membrane potential (deltapsi(m)) in apoptosis; an update. Apoptosis, 2003. 8(2): p. 115-28.
149. Seppi, T., et al., Sex Differences in Renal Proximal Tubular Cell Homeostasis. J Am SocNephrol, 2016. 27(10): p. 3051-3062.
150. Lima-Posada, I., et al., Gender Differences in the Acute Kidney Injury to Chronic Kidney Disease Transition. Scientific Reports, 2017. 7(1): p. 12270.
151. Iran-Nejad, A., et al., Preventive role of estradiol on kidney injury induced by renal ischemia-reperfusion in male and female rats. International journal of preventive medicine, 2015. 6.
152. Elliot, S.J., et al., Smoking induces glomerulosclerosis in aging estrogen-deficient mice through cross-talk between TGF-β1 and IGF-I signaling pathways. Journal of the American Society of Nephrology, 2006. 17(12): p. 3315-3324.
153. in The Health Consequences of Smoking-50 Years of Progress: A Report of the SurgeonGeneral. 2014: Atlanta (GA).
154. Bruetto, R.G., et al., Renal function at hospital admission and mortality due to acute kidney injury after myocardial infarction. PLoS One, 2012. 7(4): p. e35496.
155. Kobeissy, F., et al., Acute Exposure to Cigarette Smoking Followed by Myocardial Infarction Aggravates Renal Damage in an In Vivo Mouse Model. Oxidative Medicine and Cellular Longevity, 2017. 2017.
156. Karakaya, O., et al., Acute smoking-induced alterations in Doppler echocardiographic measurements in chronic smokers. Tex Heart Inst J, 2006. 33(2): p. 134-8.
157. M Reslan, O. and R. A Khalil, Vascular effects of estrogenic menopausal hormone therapy.Reviews on recent clinical trials, 2012. 7(1): p. 47-70.
158. Welinder, C. and L. Ekblad, Coomassie staining as loading control in Western blot analysis.Journal of proteome research, 2011. 10(3): p. 1416-1419.
159. Cruz, D.N., Cardiorenal syndrome in critical care: the acute cardiorenal and renocardiac syndromes. Advances in chronic kidney disease, 2013. 20(1): p. 56-66.
160. Virzì, G.M., et al., Cardiorenal syndrome type 1 may be immunologically mediated: a pilot evaluation of monocyte apoptosis. Cardiorenal medicine, 2012. 2(1): p. 33-42.
161. Windt, W.A., et al., Renal damage after myocardial infarction is prevented by renin-angiotensin-aldosterone-system intervention. Journal of the American Society of Nephrology, 2006. 17(11): p. 3059-3066.
162. Saha, S.P., et al., Cigarette smoke and adverse health effects: An overview of research trends and future needs. The International journal of angiology: official publication of the International College of Angiology, Inc, 2007. 16(3): p. 77.
163. Orth, S., Cigarette smoking: an important renal risk factor–far beyond carcinogenesis. Tobacco induced diseases, 2003. 1(2): p. 137.
164. Ozbek, E., Induction of oxidative stress in kidney. International journal of nephrology, 2012. 2012.
165. Hua, P., et al., Nicotine worsens the severity of nephropathy in diabetic mice: implications for the progression of kidney disease in smokers. American Journal of Physiology-Renal Physiology, 2010. 299(4): p. F732-F739.
166. Ambrose, J.A. and R.S. Barua, The pathophysiology of cigarette smoking and cardiovascular disease: an update. Journal of the American college of cardiology, 2004.

43(10): p. 1731-1737.
167. Kim, C.S., et al., Nicotine-induced apoptosis in human renal proximal tubular epithelial cells. PloS one, 2016. 11(3): p. e0152591.
168. Evans, W., T.M. Phernetton, and R.R. Magness, 17β-estradiol effect on critical cardiac output with reduction of cardiac output in oophorectomized sheep. American Journal of Physiology-Heart and Circulatory Physiology, 1998. 275(1): p. H57-H64.
169. Billon, A., et al., The estrogen effects on endothelial repair and mitogen-activated protein kinase activation are abolished in endothelial nitric-oxide (NO) synthase knockout mice,but not by NO synthase inhibition by N-nitro-L-arginine methyl ester. The American journal of pathology, 2008. 172(3): p. 830-838.
170. Dubey, R.K. and E.K. Jackson, Estrogen-induced cardiorenal protection: potential cellular, biochemical, and molecular mechanisms. American Journal of Physiology-Renal Physiology, 2001. 280(3): p. F365-F388.
171. Doublier, S., et al., Testosterone and 17β-estradiol have opposite effects on podocyte apoptosis that precedes glomerulosclerosis in female estrogen receptor knockout mice. Kidney international, 2011. 79(4): p. 404-413.
172. Arici, M. and J. Walls, End-stage renal disease, atherosclerosis, and cardiovascular mortality: is C-reactive protein the missing link? Kidney international, 2001. 59(2): p. 407-414.
173. Testa, M., et al., Circulating levels of cytokines and their endogenous modulators in patients with mild to severe congestive heart failure due to coronary artery disease or hypertension. Journal of the American College of Cardiology, 1996. 28(4): p. 964-971.
174. Niijima, A., et al., The effects of interleukin-1β on the activity of adrenal, splenic and renal sympathetic nerves in the rat. Journal of the autonomic nervous system, 1991. 36(3): p. 183-192.
175. Zhou, X., et al., Protective effects of valsartan against cigarette smoke-induced left ventricular systolic dysfunction in rats. International journal of cardiology, 2013. 167(3): p. 677-680.
176. Ridker, P.M., et al., Inhibition of Interleukin-1β by Canakinumab and Cardiovascular Outcomes in Patients With Chronic Kidney Disease. Journal of the American College of Cardiology, 2018. 71(21): p. 2405-2414.
177. Rogers, A. and R. Eastell, The effect of 17β-estradiol on production of cytokines in cultures of peripheral blood. Bone, 2001. 29(1): p. 30-34.
178. Zhang, M.-Z., et al., IL-4/IL-13–mediated polarization of renal macrophages/dendritic cells to an M2a phenotype is essential for recovery from acute kidney injury. Kidney international, 2017. 91(2): p. 375-386.
179. Yokota, N., et al., Contrasting roles for STAT4 and STAT6 signal transduction pathways in murine renal ischemia-reperfusion injury. American Journal of Physiology-Renal Physiology, 2003. 285(2): p. F319-F325.
180. Campbell, L., et al., Estrogen receptor-alpha promotes alternative macrophage activation during cutaneous repair. Journal of Investigative Dermatology, 2014. 134(9): p. 2447-2457.
181. Riffo-Vasquez, Y., et al., Role of sex hormones in allergic inflammation in mice. Clinical &

Experimental Allergy, 2007. 37(3): p. 459-470.
182. Zymek, P., et al., Interleukin-10 is not a critical regulator of infarct healing and left ventricular remodeling. Cardiovascular research, 2007. 74(2): p. 313-322.
183. Craig, V.J., et al., Profibrotic activities for matrix metalloproteinase-8 during bleomycin- mediated lung injury. The Journal of Immunology, 2013: p. 1201043.
184. García-Prieto, E., et al., Resistance to bleomycin-induced lung fibrosis in MMP-8 deficient mice is mediated by interleukin-10. PloS one, 2010. 5(10): p. e13242.
185. George, J., M. Tsutsumi, and M. Tsuchishima, MMP-13 deletion decreases profibrogenic molecules and attenuates N-nitrosodimethylamine-induced liver injury and fibrosis inmice. Journal of cellular and molecular medicine, 2017. 21(12): p. 3821-3835.
186. Meran, S. and R. Steadman, Fibroblasts and myofibroblasts in renal fibrosis. International journal of experimental pathology, 2011. 92(3): p. 158-167.
187. Moriya, C., et al., Expression of matrix metalloproteinase-13 is controlled by IL-13 via PI3K/Akt3 and PKC-δ in normal human dermal fibroblasts. Journal of Investigative Dermatology, 2011. 131(3): p. 655-661.
188. Abe, M., et al., Induction of collagenase-2 (matrix metalloproteinase-8) gene expression by interleukin-1β in human gingival fibroblasts. Journal of periodontal research, 2001.36(3): p. 153-159.
189. van der Veer, E., et al., Extension of human cell lifespan by nicotinamide phosphoribosyltransferase. Journal of Biological Chemistry, 2007. 282(15): p. 10841-10845.
190. Pillai, J.B., et al., Poly (ADP-ribose) polymerase-1 dependent cardiac myocyte cell-death during heart failure is mediated by NAD+ depletion and reduced activity of the Sir2α deacetylase. Journal of Biological Chemistry, 2005.
191. Ratajczak, J., et al., NRK1 controls nicotinamide mononucleotide and nicotinamide riboside metabolism in mammalian cells. Nature communications, 2016. 7: p. 13103.
192. Hershberger, K.A., A.S. Martin, and M.D. Hirschey, Role of NAD+ and mitochondrial sirtuins in cardiac and renal diseases. Nature Reviews Nephrology, 2017. 13(4): p. 213.
193. Zhuo, L., et al., NAD blocks high glucose induced mesangial hypertrophy via activation of the sirtuins-AMPK-mTOR pathway. Cellular Physiology and Biochemistry, 2011. 27(6): p.681-690.
194. Morigi, M., et al., Sirtuin 3–dependent mitochondrial dynamic improvements protect against acute kidney injury. The Journal of clinical investigation, 2015. 125(2): p. 715-726.
195. Kong, L., et al., Sirtuin 1: a target for kidney diseases. Molecular Medicine, 2015. 21(1): p.87.
196. Kitada, M., S. Kume, and D. Koya, Role of sirtuins in kidney disease. Current opinion in nephrology and hypertension, 2014. 23(1): p. 75-79.
197. Shen, T., et al., SIRT1 functions as an important regulator of estrogen-mediated cardiomyocyte protection in angiotensin II-induced heart hypertrophy. Oxidative medicine and cellular longevity, 2014. 2014.
198. Capllonch-Amer, G., et al., Estradiol stimulates mitochondrial biogenesis and adiponectin expression in skeletal muscle. Journal of Endocrinology, 2014: p. JOE-14-0008.